

## WIDE-FIELD SURVEY OF GLOBULAR CLUSTERS IN M31. I. A CATALOG OF NEW CLUSTERS

SANG CHUL KIM<sup>1,2,3</sup>, MYUNG GYOON LEE<sup>2,3</sup>, DOUG GEISLER<sup>3,4</sup>, ATA SARAJEDINI<sup>3,5</sup>, HONG SOO PARK<sup>2</sup>, HO SEONG HWANG<sup>2</sup>,  
WILLIAM E. HARRIS<sup>6</sup>, JUAN C. SEGUEL<sup>4,7</sup>, & TED VON HIPPEL<sup>3,8,9</sup>

*Draft version February 1, 2008*

### ABSTRACT

We present the result of a wide-field survey of globular clusters (GCs) in M31 covering a  $3^\circ \times 3^\circ$  field centered on M31. We have searched for GCs on CCD images taken with Washington *CMT*<sub>1</sub> filters at the KPNO 0.9 m telescope using the following steps: (1) inspection of morphological parameters given by the SExtractor package such as stellarity, full width at half-maximum, and ellipticity; (2) consulting the spectral types and radial velocities obtained from spectra taken with the Hydra spectrograph at the WIYN 3.5 m telescope; and (3) visual inspection of the images of each object. We have found 1164 GCs and GC candidates, of which 605 are newly found GCs and GC candidates and 559 are previously known GCs. Among the new objects there are 113 genuine GCs, 258 probable GCs, and 234 possible GCs, according to our classification criteria. Among the known objects there are 383 genuine GCs, 109 probable GCs, and 67 possible GCs. In total there are 496 genuine GCs, 367 probable GCs and 301 possible GCs. Most of these newly found GCs have  $T_1$  magnitudes of 17.5–19.5 mag, [ $17.9 < V < 19.9$  mag assuming  $(C - T_1) \approx 1.5$ ], and  $(C - T_1)$  colors in the range 1–2.

*Subject headings:* galaxies: star clusters — galaxies: spiral — galaxies: individual (M31, NGC 224) — Local Group

### 1. INTRODUCTION

Globular clusters (GCs) are an ideal tool for studying the formation and evolution of nearby galaxies for several reasons. First, GCs are one of the brightest objects in galaxies, so it is relatively easy to observe them even in the outer parts of the galaxies where individual stars are too faint to be observed. Second, GCs are believed to be among the oldest objects in galaxies (see, e.g., Salaris & Weiss (2002); De Angeli et al. (2005)) giving a lower limit to the ages of their parent galaxies. Third, the stars in GCs are believed to be born essentially at the same time and with the same chemical composition, which makes GCs an ideal laboratory for the study of stellar evolution. Fourth, GCs are distributed much more widely than stars, so they can be used for the study of the halo of their parent galaxy. Finally, since the present GCs have survived since the formation of their parent galaxies, they give information on the formation and evolution of both the clusters and the galaxies.

The GCs in M31 are especially important, since M31 is the nearest spiral galaxy and has an abundant population of GCs.

There have been numerous studies of the GCs in M31 starting as early as 1932. Table 1 shows a list of the previous studies on M31 GCs, focusing primarily on the number of GCs and candidate GCs found. Examples of the most extensive GC surveys are those of Sargent et al. (1977, the M31 Consortium), Crampton et al. (1985, the DAO group), and Battistini et al. (1987, the Bologna group). However, these surveys are mostly based on visual searches of the photographic plates.

Since the use of CCD detectors in astronomy, there have been efforts to use them for deep photometry to search for new GCs in M31. However, the small field of view (FOV) of the first generation CCDs enabled previous investigators only to perform GC surveys for a limited region of M31, and there has not yet been any wide-field survey of GCs using CCD cameras. It is clear from Table 1 that our new GC survey presented in this study is the first systematic one for the largest area of  $\sim 3^\circ \times 3^\circ$  centered on M31.

Recently several new extended GCs were found in the halo located at  $15 \lesssim R_p \lesssim 116$  kpc (where  $R_p$  is the projected radius) from the center of M31 (Huxor et al. 2005; Martin et al. 2006; Mackey et al. 2007), and Mackey et al. (2006, 2007) presented deep photometry of stars in these clusters based on *Hubble Space Telescope* (HST) ACS images. Kodaira et al. (2004) found 49 compact star clusters with  $M_V < -5$  mag and  $0 < (B - V) < 1.0$  in the south-west field ( $17'.5 \times 28'.5$ ) of the M31 disk from CCD images taken at the Subaru 8 m telescope, some of which may be GCs.

This paper is the first in a series on our wide-field survey of M31 GCs. In this paper we present a catalog of new GCs in M31, and the analyses of the photometric and spectroscopic data of the new and known GCs in M31 will be presented in separate papers. Brief progress reports of this study were given in Lee et al. (2002), Kim et al. (2002), and Seguel et al. (2002), which are superseded by this series of papers.

This paper is organized as follows: §2 describes the photometric and spectroscopic observations and data reductions, and §3 the GC search method. Section 4 presents the catalog of new GCs found in this study and some properties of newly found GCs, and finally, a summary is given in §5.

<sup>1</sup> Korea Astronomy and Space Science Institute, Daejeon 305-348, Korea; sckim@kasi.re.kr

<sup>2</sup> Astronomy Program, Department of Physics and Astronomy, Seoul National University, Seoul 151-742, Korea; mglee@astrog.snu.ac.kr, hspark@astro.snu.ac.kr, hshwang@astro.snu.ac.kr

<sup>3</sup> Visiting Astronomer, Kitt Peak National Observatory, National Optical Astronomy Observatory, which is operated by the Association of Universities for Research in Astronomy (AURA), Inc., under cooperative agreement with the National Science Foundation.

<sup>4</sup> Grupo de Astronomía, Departamento de Física, Universidad de Concepción, Casilla 160-C, Concepción, Chile; dgeisler@astro-udec.cl, jseguel@andromeda.cfm.udec.cl

<sup>5</sup> Department of Astronomy, University of Florida, Gainesville, FL 32611, USA; ata@astro.ufl.edu

<sup>6</sup> Department of Physics and Astronomy, McMaster University, Hamilton, ON L8S 4M1, Canada; harris@physics.mcmaster.ca

<sup>7</sup> Cerro Tololo Inter-American Observatory, Casilla 603, La Serena, Chile

<sup>8</sup> Department of Astronomy, University of Texas at Austin, 1 University Station C1400, Austin, TX 78712, USA; ted@astro.as.utexas.edu

<sup>9</sup> Visiting Scientist, Southwest Research Institute, 1050 Walnut Street, Suite 400, Boulder, CO 80302, USA

## 2. OBSERVATIONS AND DATA REDUCTION

We carried out two kinds of observation for the survey of M31 GCs. First, photometric observations were made using the CCD camera at the KPNO 0.9 m telescope. Second, spectroscopic observations were performed using the Hydra multi-fiber spectrograph at the WIYN 3.5 m telescope. We describe the details of these observations below.

### 2.1. Photometry

#### 2.1.1. Observation

We obtained Washington *C* and *M* and broadband Kron-Cousins *R* images using the T2KA CCD camera at the KPNO 0.9 m telescope on the nights of UT 1996 October 14 – 25 and UT 1998 October 19. The pixel scale of the CCD chip is  $0.68'' \text{ pixel}^{-1}$ , and the CCD has  $2048 \times 2048$  pixels, corresponding to  $23.2' \times 23.2'$  on the sky. We used the Kron-Cousins *R* filter as an alternative to the  $T_1$  filter, since the *R* filter accurately reproduces the  $T_1$  photometry with 3 times greater efficiency (Geisler 1996). The resulting calibrated magnitudes and colors will therefore be in the Washington  $CMT_1$  system. Geisler (1996) gave a transformation relation between *R* and  $T_1$ ,  $R = 0.003 + T_1 - 0.017(C - T_1)$ , with an rms of only 0.02 mag derived from the data of 53 standard stars.

We observed 53 fields covering the central region of M31. Figure 1 shows the location of the observed fields, the names of which are labeled in the upper left corner of each solid box. For most of the fields, one exposure per filter was made. Typical exposure times for the 1996 run were 1500 s for *C* and 600 s for *M* and *R*, while those for the 1998 run were 1200 s for *C* and 500 s for *M* and *R*. The seeing was mostly  $1.1'' - 2.0''$  ( $1.6 - 2.9$  pixels in our CCD frames) during the observations, although a few fields have a seeing of  $2.0'' - 3.0''$ . Table 2 lists the journal of observation, where column (1) is the night number, column (2) the observation date in UT, column (3) the field numbers, and column (4) the weather condition. Of the total of 11 nights of observation, four nights (N5, N8, N9 and Oct98) were photometric, three (N3, N4, and N11) were semi-photometric, and the remaining four nights were non-photometric or even cloudy. The standard star observations were made in the photometric and semi-photometric nights indicated in Table 2.

#### 2.1.2. Data Reduction

We processed all the CCD images to apply overscan correction, bias subtraction and flat fielding using the IRAF<sup>10</sup>/CCDRED package. We derived the calibration transformation using the Washington standard stars (Geisler 1996) observed during the observing runs. We obtained the aperture magnitudes of the standard stars using a  $7.5''$  radius aperture (the same as in Geisler (1996)) from the images of the standard stars. Then we used the IRAF PHOTCAL package to derive the calibration equations.

For three out of the four nights of photometric conditions, all three standard calibration coefficients (zeropoint, color term, and airmass term) were derived. For the three nights of semi-photometric conditions, we adopted the mean values of the color and airmass term coefficients of the three photometric nights to derive the zeropoints. Although the night of UT 1996 October 22 was believed to be photometric, there were

not enough standard stars to derive all three calibration coefficients independently, so we adopted the color and airmass term coefficients of the previous photometric night.

For the fields observed on the nights without standard stars, we derived secondary standard transformations using the neighboring fields. Since we initially arranged our target fields to overlap adjacent fields by  $1' - 2'$ , we could easily identify the stars in common between two neighboring fields. On the image of each filter, we first identified the positions of the common stars in the two adjacent fields, calculated the mean magnitude offsets between the standardized magnitudes and instrumental magnitudes, and then applied this magnitude offset (together with the color and atmospheric coefficients of the standardized field) to transform the instrumental magnitudes of the nonphotometric frames. There are 14 fields for which this secondary transformation method is applied. The typical errors of the standard star calibration are 0.020, 0.022, and 0.019 mag for  $T_1$ ,  $(C - T_1)$ , and  $(M - T_1)$ , respectively.

We have derived the photometry of the objects in the target images using the SExtractor package (Bertin & Arnouts 1996). SExtractor performs detection of objects in the images and gives position, aperture magnitude, stellarity, the full width at half-maximum (FWHM), ellipticity, position angle, quality of the photometry, and some other parameters. We used the SExtractor parameters DETECT\_MINAREA = 5 pixel and DETECT\_THRESH =  $1.5\sigma$  above the local background. The results for new GC searches do not depend strongly on the choice of these values. The instrumental magnitudes of the objects obtained using the SExtractor package were transformed into the standard system using the calibration equations.

We have obtained plate solutions for each of the CCD images for astrometry of objects using the Guide Star Catalogue (GSC) provided by the Space Telescope Science Institute (STScI) and the IRAF tasks CCXYMATCH and CCMAP. These plate solutions transform the *X* and *Y* coordinates of our *R* images to/from the celestial equatorial coordinates of epoch J2000.0 by using the IRAF CCTRAN task. The mean rms errors in right ascension and declination are  $0.064'' \pm 0.023''$  and  $0.064'' \pm 0.024''$ , respectively.

### 2.2. Spectroscopy

#### 2.2.1. Observation

For most of the GC candidates selected from the photometric list of the objects to be described in the next section, we carried out spectroscopic observation using the Hydra multi-fiber bench spectrograph and T2KC CCD at the WIYN 3.5 m telescope on the nights of UT 2000 September 7–9 and UT 2001 November 2–4. Table 3 lists the journal of spectroscopic observations. Table 3 shows the observation date in UT, the number of target objects, and the exposure time for each Hydra configuration marked in Figure 1.

For both the 2000 and 2001 observations, almost the same instrumental setup was used. The 400@4.2 grating and Simons camera were used. This combination with the blue fiber cable covers a wavelength range of  $\sim 3400 - 6600 \text{ \AA}$  in the first order and gives a  $7.07 \text{ \AA}$  spectral resolution and  $1.56 \text{ \AA pixel}^{-1}$  dispersion.

During the observing run of 2000, all three nights were clear and a total of eight Hydra configurations were used for spectroscopy. However, in the run of 2001 only the first night was clear, while the two subsequent nights were cloudy or rainy. Only three Hydra configurations were obtained during

<sup>10</sup> IRAF(Image Reduction and Analysis Facility) is distributed by the National Optical Astronomy Observatory, which is operated by AURA, Inc., under cooperative agreement with the National Science Foundation.

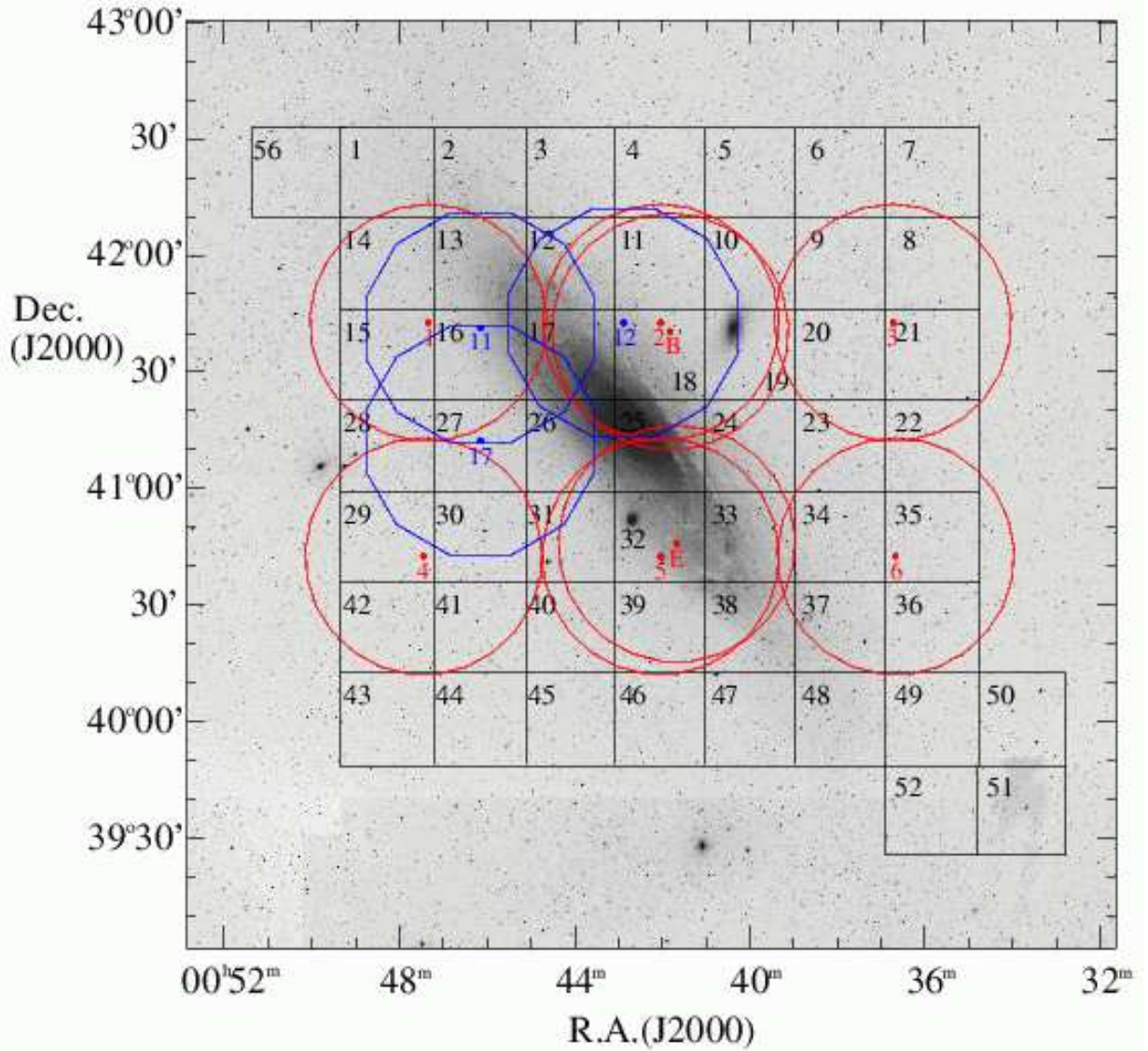


FIG. 1.— Locations of our survey regions overlaid on a  $4^\circ \times 4^\circ$  optical image of M31 from the Digitized Sky Survey (image center : R.A.(J2000.0)=  $0^h 42^m 15^s$ , Dec. (J2000.0)=  $+41^\circ 00' 37''$ ). North is at the top and east is to the left. The fields for the KPNO 0.9 m photometric imaging are drawn with solid boxes with the field names labeled in the upper left corner of each box. The field of view of each field is  $23.2' \times 23.2'$  and the observations were made so that there was some ( $1' - 2'$ ) overlap between adjacent fields. Satellite galaxies NGC 205 and M32 are located in fields 19 and 32, respectively. The Hydra fields are denoted by smooth circles (for 2000) and polygon-like circles (for 2001), and their names are labelled near the center of each field.

this run. The total number of targets observed during the observing runs was 748, including 106 previously known GCs observed in order to quantify our errors and compare our values with previous studies.

### 2.2.2. Data Reduction

First we performed overscan correction, image trimming, bias subtraction, and flat combining on the spectroscopic data using the IRAF CCDRED package. We removed cosmic rays in the object images and combined the resulting object images. For the reduction of the Hydra spectroscopic data, we used the Hydra data reduction task, IRAF DOHYDRA, which was specifically designed for multifiber spectral reduction (Valdes 1995).

Before doing the main data reduction part, DOHYDRA first performs aperture finding using the APFIND task, and per-

forms fitting and subtracting of the scattered light using the APSCATTER task. Then DOHYDRA performs aperture extraction, flat-fielding, fiber throughput correction, wavelength calibration, and sky subtraction. Dome-flat images were used as a template to extract the one-dimensional object and calibration spectra from the two-dimensional images. Cu/Ar calibration lamp spectra were used for wavelength calibration. The rms error of the wavelength calibration is estimated to be typically  $0.2 - 0.3 \text{ \AA}$ . Finally, we calibrated the flux of the spectra of the targets using the spectra of the flux standard star BD +40 4032 (R.A.(B1950)=  $20^h 06^m 40^s.0$ , Dec.(B1950)=  $+41^\circ 06' 15''$ , B2 III,  $m_{5556} = 10.45$  mag; Strom (1977)) using the CALIBRATE task.

We determined the radial velocity of the targets by cross-correlating their spectra against high signal-to-noise ratio (S/N) template spectra using the IRAF FXCOR task (Tonry

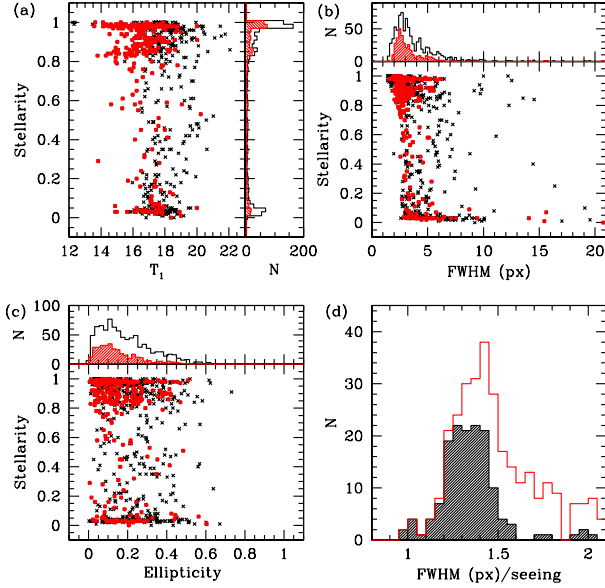


FIG. 2.—SEExtractor parameter distributions of the 347 confirmed and 514 candidate GCs in the catalogs of Galleti et al. (2006, RBC2), Huxor et al. (2005), and Mackey et al. (2007) matched with our photometry. (a) Stellarity vs.  $T_1$  magnitude; (b) stellarity vs. FWHM; (c) stellarity vs. ellipticity; (d) histogram of FWHM/seeing distribution. In panels (a), (b), and (c), the crosses and the open solid histograms show the distributions of all 861 objects with good photometry, and the filled circles and hatched histograms show those of the 347 confirmed GCs. In panel (d), the open solid histogram shows the distribution of the 347 confirmed GCs and the hatched histogram the 147 confirmed compact GCs with stellarity  $> 0.95$ .

& Davis 1979; Huchra, Brodie, & Kent 1991). We used two bright GCs in M31 as a reference. GCs 020-073 and 158-213 are relatively bright clusters with  $V = 14.91$  mag and  $(B - V) = 0.83$  and  $V = 14.70$  mag and  $(B - V) = 0.86$ , respectively, and have well-determined radial velocities of  $V_r = -349 \pm 2$  and  $-183 \pm 4$  km s $^{-1}$ , respectively (Barmby et al. 2000). We used the wavelength range of 3900 – 5400 Å for velocity measurement, excluding the noisy region of  $\lambda > 5500$  Å due to some sky lines not completely eliminated even after sky subtraction. Measuring errors of the radial velocity are typically  $err(v) = 35$  km s $^{-1}$ . For the objects with successfully measured velocity values, we measured the S/N values at  $\lambda \sim 5000$  Å, obtaining  $1 < S/N < 75$ . The peak S/N values are 6 – 10 for all these spectra, and 10 – 20 for newly found, highest probability GCs.

### 3. CLUSTER SEARCH METHOD

We have used both photometric and spectroscopic information to select GCs in M31. First, using photometric data, we investigated various photometric parameters and morphological properties of the objects in the CCD images. Then we assigned spectral classes to bright objects, and used the radial velocities to determine the M31 membership of the objects with measured radial velocities. Finally, we performed the final classification by careful visual inspection of the image of each object, after training our eyes with images of the previously known GCs, stars, and galaxies in our own data. Details of these steps are described below.

Before starting a survey of M31 GCs, we tried to find the suitable parameter space to select M31 GC candidates using the photometric data of the known M31 GCs. We matched our

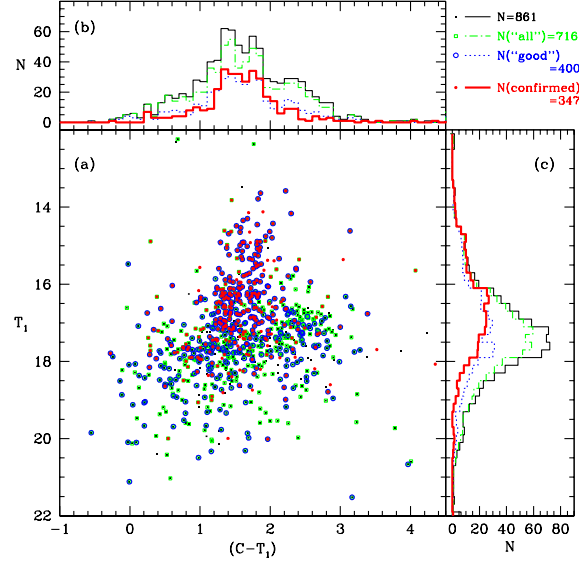


FIG. 3.—(a) Color-magnitude diagram; (b)  $(C - T_1)$  color distribution; (c)  $T_1$  LF of the 347 confirmed and 514 candidate GCs in the catalogs of Galleti et al. (2006, RBC2), Huxor et al. (2005), and Mackey et al. (2007) matched with our photometry. Small dots and thin solid histograms show the distributions of all 861 objects with good photometry, open squares and dot-dashed histograms show the distributions of “all GC candidates” from the GC search criterion 1, open circles and dotted histograms show the distributions of “good GC candidates” from criterion 2, and filled circles and thick solid histograms show the distributions of the confirmed GCs in the three papers above.

photometric catalog of the objects with the previous catalogs of Galleti et al. (2006) (Revised Bologna Catalog ver. 2.0 [RBC2] – their confirmed and candidate GCs), Huxor et al. (2005), and Mackey et al. (2007). There are 861 objects (347 confirmed GCs and 514 GC candidates) common between the previous catalogs and our catalog of photometry derived from our CCD images.

Figure 2 shows the distributions of three SEExtractor parameters (stellarity, FWHM and ellipticity) based on the  $R$  images, and Figures 3 and 4 show the photometric diagrams of these objects. In Figure 2 (a), (b), and (c), the crosses and the open solid histograms show the distributions of all 861 objects with good photometry, and the filled circles and hatched histograms show those of the confirmed GCs in common between this study and the papers above. As stellarity of 1 corresponds to a point-source (star), and a stellarity of 0 to a resolved object. The distribution of stellarity in Figure 2 shows that most objects have stellarity of 1, few objects have stellarity between 0.1 and 0.8, and the rest have stellarity  $\sim 0$ . Figure 2 (d) shows the histogram of the normalized FWHM, which is the measured FWHM divided by the seeing value of each image.

In Figure 2 several features are noted: (1) the distribution of the stellarity of the confirmed GCs shows a strong peak around 1 with a broad tail extending to about 0.8, and a weak peak around 0. There are relatively much fewer GCs in the range between 0.1 and 0.8; (2) the distribution of the ellipticity of the confirmed GCs shows a broad peak around 0.1 with a tail extending to 0.5; and (3) the distribution of the normalized FWHM of the confirmed GCs shows a strong peak around 1.4, which is significantly larger than that of the stars, 1.0. Considering the pixel scale of our CCD chip, typical see-



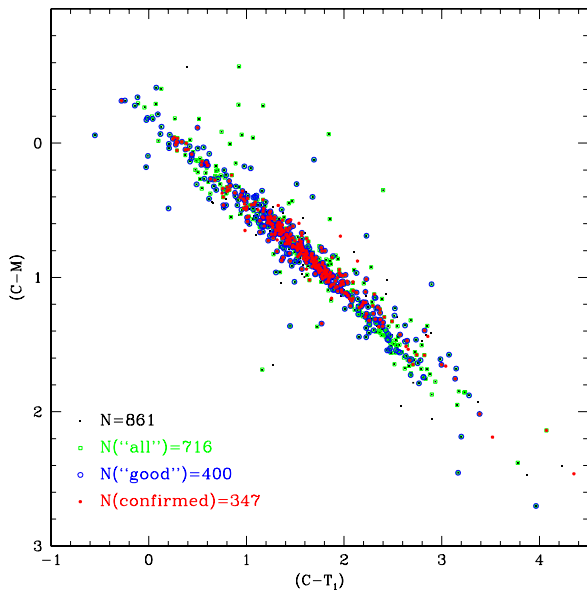


FIG. 4.— Color-color diagram of the 347 confirmed and 514 candidate GCs in the catalogs of Galleti et al. (2006, RBC2), Huxor et al. (2005), and Mackey et al. (2007) matched with our photometry. Small dots show the distributions of all 861 objects with good photometry, open squares show the distributions of “all GC candidates” from the GC search criterion 1, open circles show the distributions of “good GC candidates” from criterion 2, and filled circles show the distributions of the confirmed GCs in the three papers above.

ing of 2 pixels ( $\approx 1''.4$ ), and the linear size of  $1''$  at the distance of M31 ( $\approx 3.78$  pc), it is expected that most of the GCs in M31 will appear point-source-like. Even for these star-like GCs, Figure 2 (d) shows that the normalized FWHM is greater than 1.

Considering the features in Figure 2, we have set up two kinds of criteria for the selection of GC candidates: (1) criteria for “all candidates” are (a) all values of stellarity, (b)  $1.15 < \text{FWHM}/\text{seeing} \lesssim 10$ , and (c) ellipticity  $< 0.7$ ; and (2) criteria for “good candidates” are (a) stellarity of  $0.8-1.0$ , (b)  $1.15 < \text{FWHM}/\text{seeing} \lesssim 5$ , and (c) ellipticity  $< 0.5$ . “Good candidates” are candidates with higher probability among “all candidates.” Figure 3 shows the  $T_1 - (C - T_1)$  color-magnitude (CM) diagram (Fig 3 (a)), the histograms of  $(C - T_1)$  color (Fig 3 (b)) and  $T_1$  magnitude (Fig 3 (c)) of the 861 objects matched with the previous catalogs. Figure 4 shows the  $(C - M) - (C - T_1)$  color-color (CC) diagram of the same objects. Notable features in Figures 3 and 4 are that (1) the colors of the confirmed GCs are mostly in the range  $1 < (C - T_1) < 2$ , (2) the luminosity function (LF) of the confirmed GCs shows a peak at  $T_1 \approx 17$  mag, (3) the CM diagram shows a dominant vertical plume of GCs with  $1 < (C - T_1) < 2$  extending up to  $T_1 \sim 13.5$ , and (4) the CC diagram shows a well-defined linear sequence of star clusters.

In Figures 3 and 4 we also plotted the data for “all candidates” and “good candidates”. It is striking that the general properties of these candidates seen in these figures are very similar to those of the confirmed GCs, noting that no information of color and magnitude was used for selecting these candidates. This indicates that a significant fraction of these candidates may be GCs.

We selected the candidates in the best-seeing image among

the  $C$ ,  $M$ , and  $R$  images, which are predominantly the  $R$ -band images. We used objects at least  $\sim 1$  mag brighter than the limiting magnitude where the stellarity cannot be used to separate stellar/non-stellar objects. The typical limiting magnitude of the images is  $T_1 = 22-23$  mag, varying from field to field due to the seeing and the crowding in the field. We set the magnitude cut-off value for the candidate selection  $1-2$  mag brighter than the limiting magnitude of the images, depending on the seeing and the crowding in the images. The magnitude cut-off value for the candidate selection ranges from  $T_1 \sim 17.5$  mag (for the center field) to  $\sim 19.5$  mag (for halo fields or good seeing), mostly  $T_1 \sim 19$  mag. Therefore our search is considered to be incomplete at  $T_1 > 19$  mag for most fields (at  $T_1 > 17.5$  mag for the central field). Figure 5 shows an example of our application of the above criteria to one of the KPNO fields (F56) with a seeing of  $\approx 1.9$  pixels. In this field, there are 4894 measured objects with good photometry. Among these we selected 362 “all GC candidates” according to criterion (1), and 277 “good GC candidates” according to criterion (2).

Finally we marked the “all” and “good” GC candidates selected above on the images, and visually inspected their images to finalize the GC candidates. We checked contour maps and radial profiles of the objects as well as the images themselves. In the contour map, we classified irregular, significantly elongated, asymmetric, and loosely concentrated objects as galaxies, and round, slightly elongated, strongly concentrated objects as star clusters. Although some faint galaxies look round in the displayed images, in the contour maps their outer areas look irregular, while star clusters look very smooth and round. Inspection of the contour maps was very efficient in selecting galaxies. In the radial profile, the objects with FWHM larger than the seeing size are considered as GCs, those with FWHM similar to seeing size as stars, and those with a large excess in the wing as galaxies. Checking color, position, and/or velocity information was also included. There are some confusing cases: compact elliptical galaxies versus GCs, compact GCs versus stars, and compact star clusters in H II regions versus galaxies. For these cases spectroscopic information was needed for classification. In the outer areas close to the edge of each CCD image, the FWHMs get larger due to image degradation. Therefore, we carefully compared potential targets in these areas with other nearby objects to see whether they are really extended.

Spectral information was also used for the classification of bright objects. We have visually classified the flux-calibrated spectra into stars, star clusters, and galaxies, comparing them with the template spectra of the spectral library of Santos et al. (2002). We used the continuum of the  $4000-7000$  wavelength range as well as various spectral features: Balmer lines between  $4000$  and  $5000$  for early-type objects; absorption lines like Ca II H and K, CH (G band), MgH+MgB, and TiO for late-type objects; and emission lines for galaxies. Figure 6 displays sample spectra for confirmed GCs, young star clusters, foreground stars (F, G, and K types), and three galaxies (M31, M32 and a background galaxy).

The radial velocities were used as a strong constraint on the membership of the objects belonging to the Galaxy, M31, or the distant universe. Most of the objects with radial velocities less than  $-200$  km s $^{-1}$  are probably M31 members, while those from  $-200$  to  $+200$  km s $^{-1}$  could be M31 members or Galactic foreground stars. We considered all the objects with  $v < -300$  km s $^{-1}$  to be M31 members. The objects with  $v > 300$  km s $^{-1}$  were classified as background galaxies.

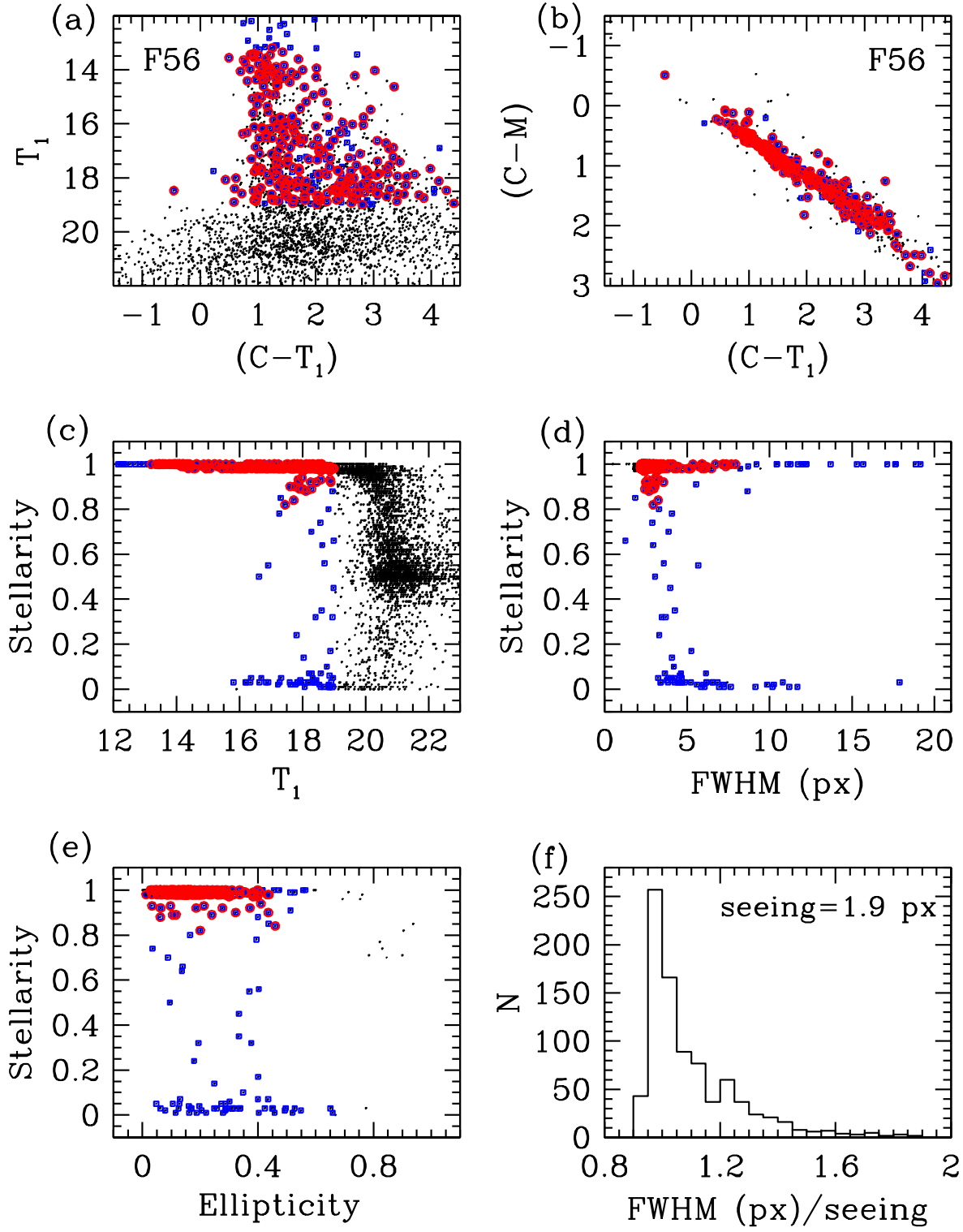


FIG. 5.— Example of our application of the GC search criteria to one of the KPNO fields (F56) with seeing of  $\approx 1.9$  pixels. Panels (a) and (b) show the CM diagram and CC diagram of the selected GC candidates, respectively, and panels (c) – (f) show the parameter space for the GC candidate selection (see Section 3 for details). Small dots represent all measured objects with good photometry ( $N=4894$ ), squares are “all GC candidates” selected according to criterion 1 ( $N=362$ ), and open circles superimposed on the squares represent “good GC candidates” selected according to criterion 2 ( $N=277$ ).

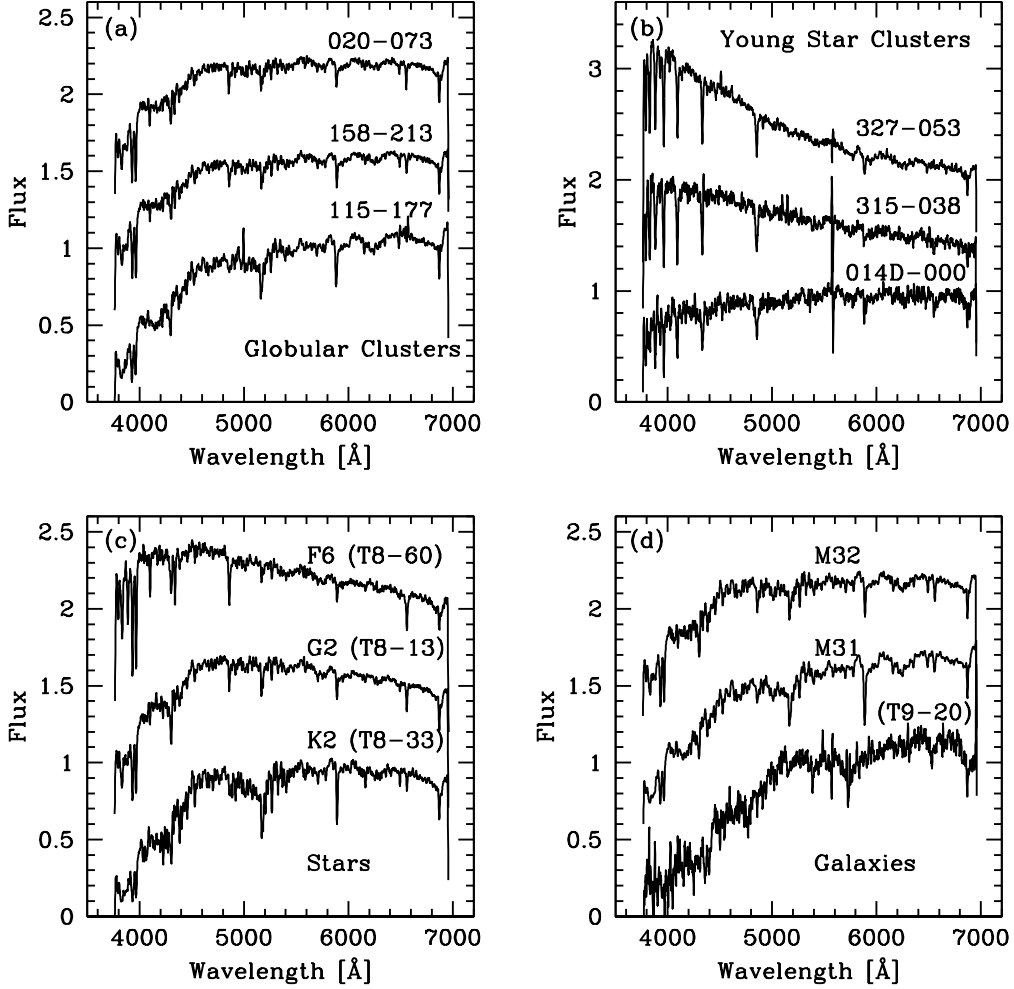


FIG. 6.— Sample spectra of (a) M31 globular clusters, (b) M31 young star clusters, (c) foreground stars, and (d) three galaxies (M31, M32 and a background galaxy). We have followed Huchra, Brodie, & Kent (1991) and Barmby et al. (2000) for the naming convention of M31 GCs. The numbers after T8- and T9- in the parentheses of panels (c) and (d) are the identification numbers in Tables 16–17 and 18, respectively.

For objects with  $-300 \text{ km s}^{-1} < v < +300 \text{ km s}^{-1}$ , we classified each object consulting its spectral class.

Combining both image and spectral inspections was very efficient and accurate in classifying the objects. For our fields F08–F42, we used both image inspection and spectral inspection methods, while for the fields without spectroscopic data (F1–F7, F43–F52, and F56) we used only the image inspection method.

We have classified the final GCs/GC candidates into three classes according to probability as follows: (1) class 1, genuine GCs that were confirmed by either spectral types and radial velocities or high resolution images (mostly *HST* images); (2) class 2, probable clusters that are probably GCs from imaging data but without spectral information; and (3) class 3, possible clusters that are possibly GCs, but may be other kinds of objects like background galaxies.

#### 4. RESULTS

##### 4.1. The Catalog of New Globular Clusters in M31

By applying the cluster search method described in the previous Section to the 53 KPNO fields of M31 covering a  $\sim 3^\circ \times 3^\circ$  area, we have found a total of 1164 GC candidates. Among these there are 605 new GC candidates found in this study and 559 previously known GCs in the catalogs of previous studies (e.g., Huxor et al. (2005); Galleti et al. (2006); Mackey et al. (2007)). Table 4 lists a summary of the numbers of the GCs and GC candidates for each class. Among the new 605 GC candidates there are 113 genuine GCs (class 1), 258 probable GCs (class 2) and 234 possible GCs (class 3). Among the known GCs in previous studies we find 383 genuine GCs, 109 probable GCs and 67 possible GCs. In total there are 496 genuine GCs, 367 probable GCs and 301 possible GCs.

Tables 5–6, 7–11, and 12–15 present the lists of the GCs and GC candidates newly found in this study for genuine GCs, probable GCs, and possible GCs, respectively. In these tables the columns give the running number (col. [1]), the coordinates in right ascension and declination (J2000.0; cols. [2] and [3]),  $T_1$  magnitudes (col. [4]),  $(M - T_1)$  and  $(C - T_1)$  colors (cols. [5] and [6]), and the radial velocities derived in this study (col. [7]). The magnitudes and colors here are from the simple aperture photometry derived using SExtractor with an aperture of radius  $5''$ . Figures 7, 8, and 9 show the *R*-band mosaic images of genuine GCs (class 1) with identifications in Tables 5–6 labeled.

Tables 16–17 and 18 present the lists of 111 stars and 21 galaxies, respectively, identified in the present study. The columns are the same as those of Tables 5–6, except the last column of Table 18, which gives the identification matched with the RBC2 of Galleti et al. (2006). These lists of stars and galaxies were obtained from the spectral classification described in Section 3. We found that 13 objects in these lists were already identified as galaxies or GC candidates without measured velocities in the RBC2 catalog.

##### 4.2. Properties of New Globular Clusters

Although the detailed properties of the newly found GCs/GC candidates as well as those of the whole M31 GC system including the previously known GCs will be presented in separate papers, we show a few salient features of the newly found objects here.

Figure 10 shows the  $T_1 - (C - T_1)$  CM diagram (Fig. 10 (a)),  $(C - T_1)$  color distributions (Fig. 10 (b)), and  $T_1$  LF (Fig. 10

(c)) of the newly found GCs/GC candidates in Tables 5–6, 7–11, and 12–15. Figure 11 shows the  $(C - M) - (C - T_1)$  CC diagram of the same objects. Most of the class 1 GCs have  $T_1$  magnitudes of 17.5–19.5 mag, which would be  $V \approx 17.9 - 19.9$  mag assuming  $(C - T_1) \approx 1.5$  (see below) and using the Geisler (1996)'s transformation coefficients between *UBVRI* photometry and  $CT_1$  photometry. Figure 12 shows the direct comparison of the confirmed, previously known GCs and newly found, class 1 GCs in the  $T_1 - (C - T_1)$  CM diagram, and it is noted that most of the class 1 GCs newly found in this study are fainter than most of the confirmed, previously known GCs. The brightest object among the newly found class 1 GCs has  $T_1 \sim 14.6$  ( $V \sim 15.0$ ) mag and the faintest one has  $T_1 \sim 19.9$  ( $V \sim 20.1$ ) mag. We checked the color distributions of the previously known GCs and newly found GCs, confirming that they are quite similar.

Figure 10 (b) shows that the  $(C - T_1)$  color distributions of all three classes encompass the color range of  $1 < (C - T_1) < 2$  [ $0.6 \lesssim (B - V) \lesssim 1.0$ ; Geisler (1996)], in which most of the class 1 objects reside. There are a rather large number of very red objects with  $2 < (C - T_1) < 2.5$  [ $(B - V) \approx 1.0 - 1.3$ ], which could be reddened GCs or intrinsically red clusters.

Figure 13 shows the spatial distribution and histograms of the newly found GCs and GC candidates. Open circles and filled histograms are for class 1 GCs in this study, crosses are for class 2 GCs in this study, and dots and open solid histograms are for GCs in the catalogs of Galleti et al. (2006, their class 1), Huxor et al. (2005), and Mackey et al. (2007). Most of the newly found, class 1 GCs are located in the disk area of M31. Higher spatial resolution imaging and spectroscopy, and possibly in the near-infrared wavelength band, would be needed to search for GCs in the central region of M31 where we missed many faint GCs, as seen in Figure 13 (top).

#### 5. SUMMARY

We have presented the results of a new systematic wide field CCD survey of M31 GCs. Using Washington  $CMT_1$  CCD images obtained at the KPNO 0.9 m telescope and spectra obtained using the WIYN 3.5 m telescope and Hydra multifiber bench spectrograph, we have investigated the photometric and morphological parameters of the objects, visually checked their images, and obtained their spectra and radial velocities. Finally, we have found 1164 GCs and GC candidates, of which 559 are previously known GCs and 605 are newly found GC candidates. Among the new objects there are 113 genuine GCs (class 1), 258 probable GCs (class 2), and 234 possible GCs (class 3). Among the previously known objects there are 383 genuine GCs, 109 probable GCs and 67 possible GCs. In total there are 496 genuine GCs, 367 probable GCs and 301 possible GCs.

The magnitudes and colors of most of the newly found class 1 objects are  $17.5 < T_1 < 19.5$  mag and  $1 < (C - T_1) < 2$ . The faintest part of the M31 GC LF is mostly filled with these new GC candidates, although the intrinsically very faint GCs like AM 4, Palomar 1, E 3, and Palomar 13 in the Galaxy (see, e.g., van den Bergh & Mackey (2004); Sarajedini et al. (2007)) may remain to be detected.



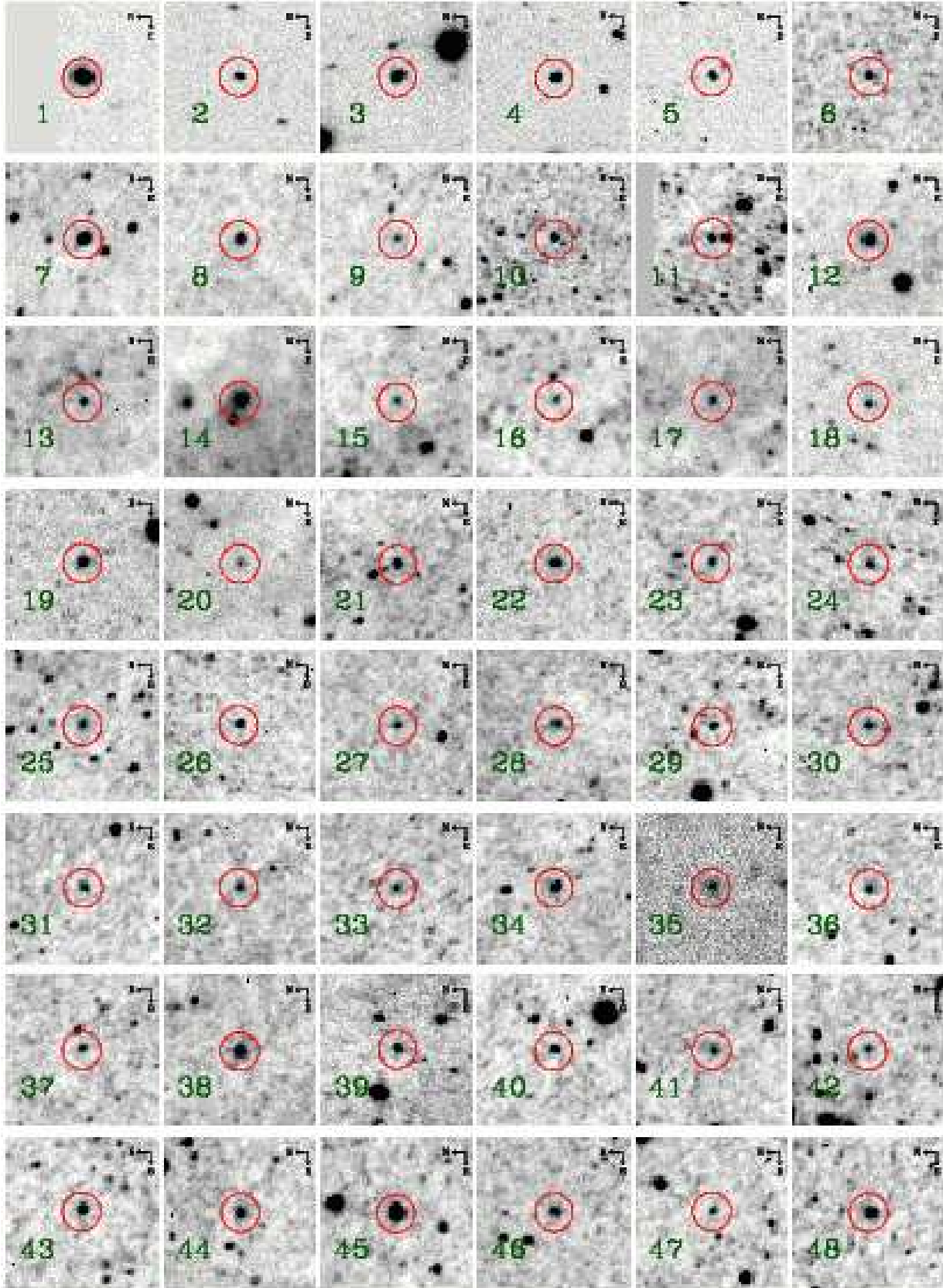


FIG. 7.— Gray-scale mosaic maps of the *R*-band CCD images of genuine GCs (class 1) for identifications from 1 to 48 in Tables 5–6. The size of each field is  $40'' \times 40''$ , with north to the left and east at the bottom. The GC is centered in each image, in the center of the circle of  $5''$  radius.

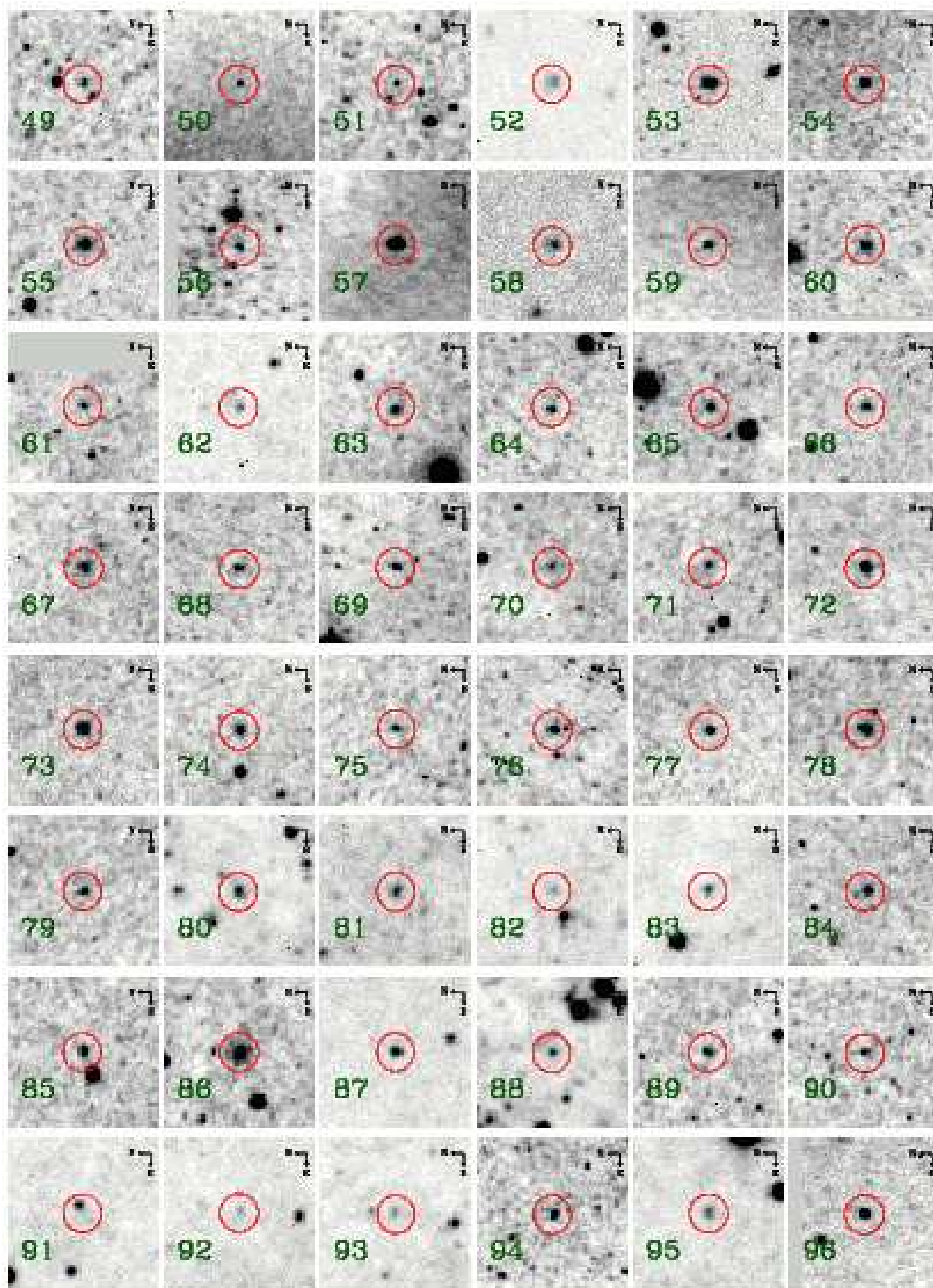


FIG. 8.— Same as Figure 7, but for identifications from 49 to 96.

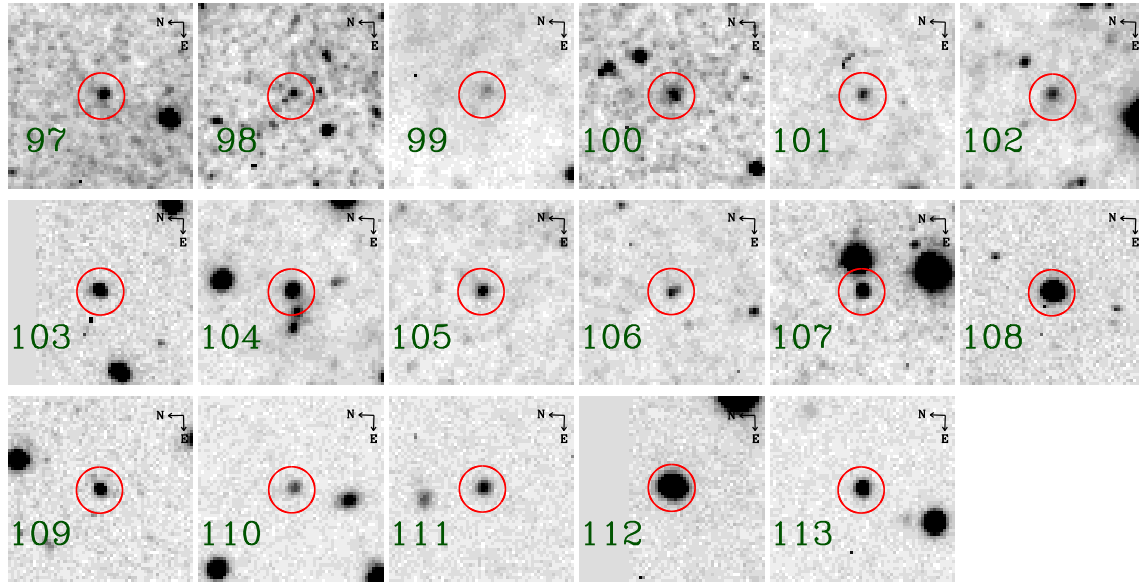


FIG. 9.— Same as Figure 7, but for identifications from 97 to 113.

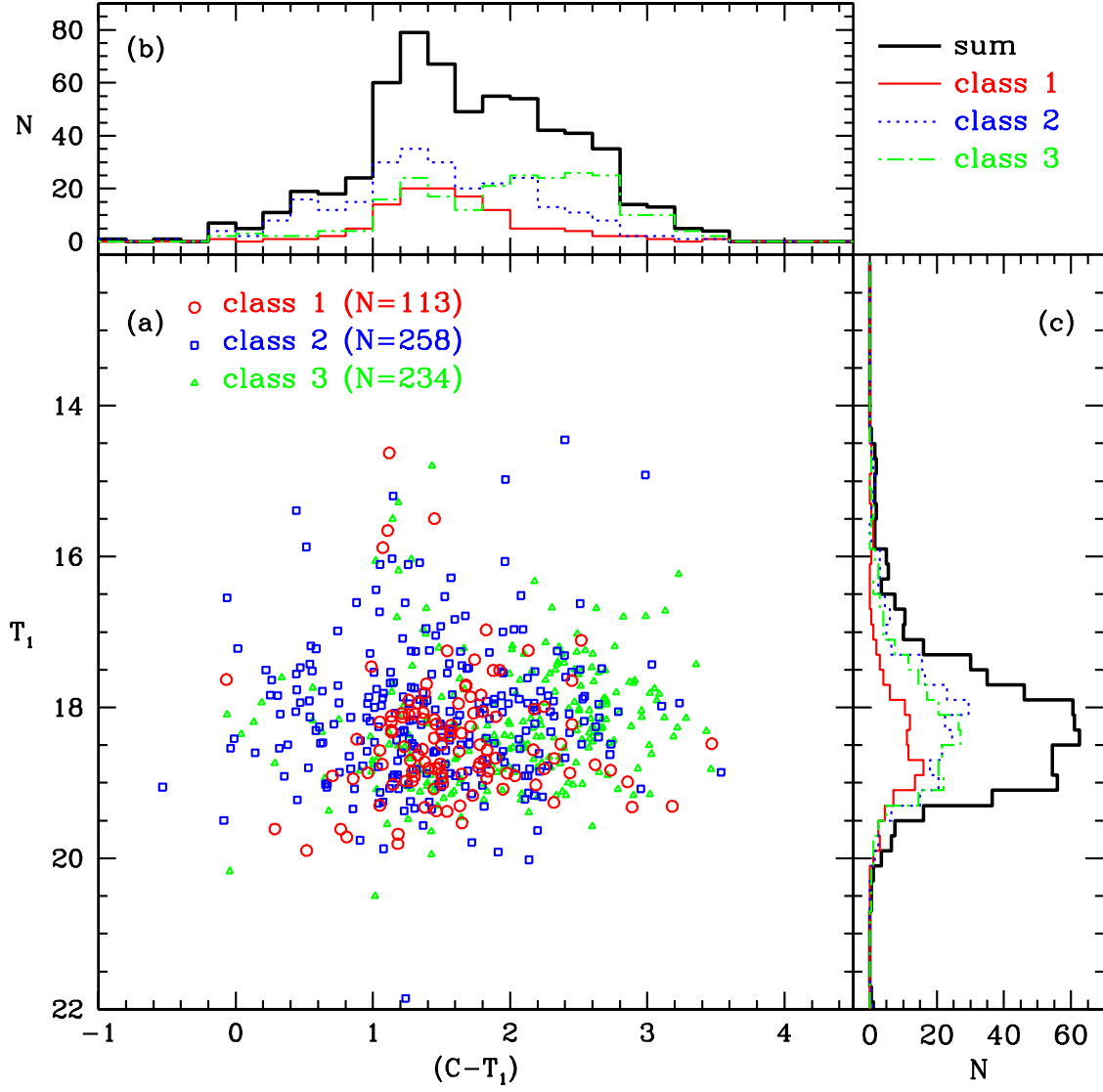


FIG. 10. — Photometric diagrams of the three classes of GCs/GC candidates newly found in this study. (a)  $T_1 - (C - T_1)$  diagram; (b)  $(C - T_1)$  color distribution; (c)  $T_1$  LF. Open circles and thin solid histograms are for genuine GCs (class 1), open squares and dotted histograms are for probable GCs (class 2), and open triangles and dot-dashed histograms are for possible GCs (class 3). Thick solid histograms in panels (b) and (c) are the sum of the numbers of all three classes.

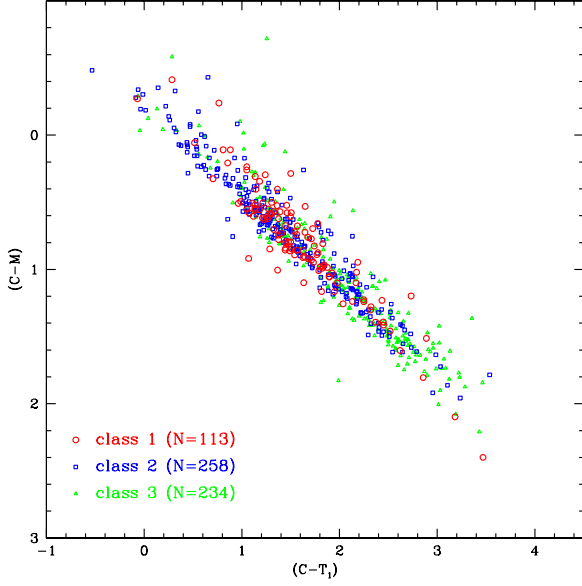


FIG. 11.—  $(C-M)-(C-T_1)$  diagram of the three classes of GCs/GC candidates newly found in this study. Open circles are for genuine GCs (class 1), open squares are for probable GCs (class 2), and open triangles are for possible GCs (class 3).

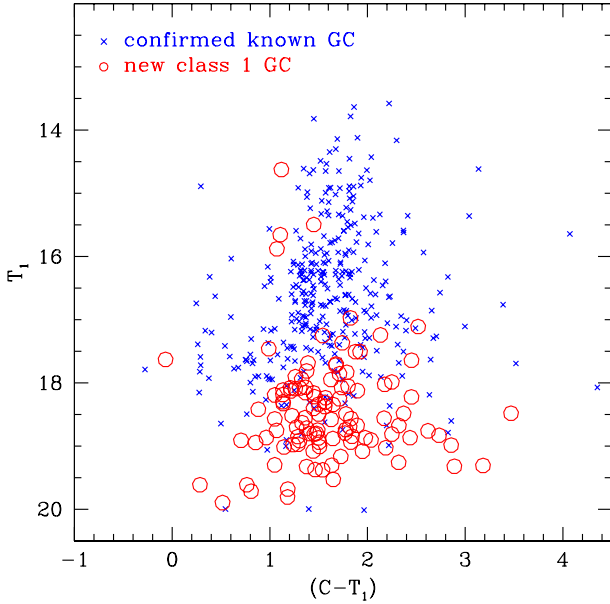


FIG. 12.—  $T_1-(C-T_1)$  CM diagram of confirmed, previously known GCs in Figure 3 (a) (crosses) and newly found, class 1 GCs in Figure 10 (a) (open circles).

We would like to thank the anonymous referee for providing prompt and thoughtful comments that helped improve the original manuscript. The authors are grateful to the staff members of the KPNO for their warm support during our observations and data reduction. The WIYN Observatory is a joint facility of the University of Wisconsin-Madison, Indiana University, Yale University, and the National Optical As-

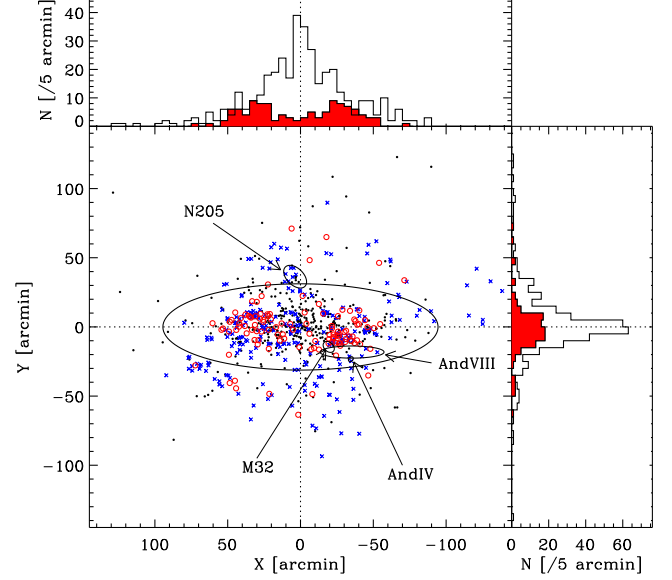


FIG. 13.— Spatial distribution and histograms of the newly found GCs and GC candidates.  $X$  is the distance measured parallel to the major axis of M31 increasing to the north-east direction, and  $Y$  is the distance parallel to the minor axis. The large ellipse is for M31 with position angle  $37.7^\circ$  (Racine 1991). The positional data of the galaxies are from Karachentsev et al. (2004), while those for And VIII are from Morrison et al. (2003). Open circles are for class 1 GCs in this study, crosses are for class 2 GCs in this study, and dots are for GCs in the catalogs of Galleti et al. (2006, their class 1), Huxor et al. (2005), and Mackey et al. (2007). The filled histograms are for class 1 GCs in this study, and the open solid histograms are for GCs in the three papers above.

tronomy Observatory. M. G. L. was supported in part by a Korean Research Foundation grant (KRF-2000-DP0450) and ABRL (R14-2002-058-01000-0). D. G. gratefully acknowledges support from Chilean Centro de Astrofísica FONDAP grant 15010003. A. S. was supported by NSF CAREER grant AST 00-94048.

#### REFERENCES

- Alloin, D., Pelat, D., & Bijaoui, A. 1976, *A&A*, 50, 127 (Erratum 1977, *A&A*, 54, 321)
- Aurière, M., Coupinot, G., & Hecquet, J. 1992, *A&A*, 256, 95
- Baade, W., & Arp, H. C. 1964, *ApJ*, 139, 1027
- Barmby, P., Huchra, J. P., Brodie, J. P., Forbes, D. A., Schroder, L. L., & Grillmair, C. J. 2000, *AJ*, 119, 727
- Barmby, P., & Huchra, J. P. 2001, *AJ*, 122, 2458
- Battistini, P., Bönoli, F., Braccetti, A., Federici, L., Fusi Pecci, F., Marano, B., & Börgen, F. 1987, *A&AS*, 67, 447
- Battistini, P., Bönoli, F., Casavecchia, M., Ciotti, L., Federici, L., & Fusi Pecci, F. 1993, *A&A*, 272, 77
- Bertin, E., & Arnouts, S. 1996, *A&AS*, 117, 393



TABLE 1  
A LIST OF PREVIOUS M31 GC SEARCHES

Reference	Plate vs. CCD	CCD FOV	N(GC)	Comments
Hubble (1932)	plate	...	140	M31's disk only
Seyfert & Nassau (1945)	plate	...	101	W. Baade's discovery, no coordinates
Vetešník (1962)	plate	...	(241) <sup>a</sup>	coordinates, <i>V</i> magnitudes and colors
Baade & Arp (1964)	plate	...	30	
Mayall & Eggen (1953)	plate	...	4	outer parts of M31
Alloin, Pelat, & Bijaoui (1976)	plate	...	5	nuclear region of M31
Sargent et al. (1977)	plate	...	355	KPNO 4 m
Crampton et al. (1985)	spectra plates	...	109	CFHT 3.6 m, A catalog of total 509 GCs
Battistini et al. (1987)	plate	...	353 <sup>b</sup>	Bologna 1.52 m
Wirth, Smarr, & Bruno (1985)	video camera	2' × 2'	~ 50	bulge region
Aurière, Coupinot, & Hecquet (1992)	CCD	1'.7 × 2'.7	16 <sup>c</sup>	7'.7 × 7'.7 field centered on M31
Battistini et al. (1993)	CCD	320 × 512 pixel <sup>2</sup>	4 <sup>d</sup>	$R < 5'.5$ ( $R \lesssim 1$ kpc)
Mochejska et al. (1998)	CCD	11' × 11'	4 <sup>e</sup>	four fields in the M31's disk
Barmby et al. (2000)	CCD	22' × 22'	(435) <sup>f</sup>	A new catalog of "best" photometry
Barmby & Huchra (2001)	HST/WFPC2	~ 2'.7 × 2'.7	32	157 images
Perrett et al. (2002)	spectroscopy	...	(288) <sup>g</sup>	WHT 4.2 m + WYFFOS
Galleti et al. (2004)	2MASS/NICMOS3	all sky	(693) <sup>h</sup>	Revised Bologna Catalogue of 1035 objects
Huxor et al. (2005)	CCD	~ 0.29deg <sup>2</sup>	3	INT 2.5 m + WFC
Galleti et al. (2006)	spectroscopy	...	(42) <sup>i</sup>	Revised Bologna Catalogue V2.0
Mackey et al. (2006, 2007)	HST/ACS	~ 3'.4 × 3'.4	14	HST Program GO 10394 (Cycle 13)
This study	CCD	23'.2 × 23'.2	605 <sup>j</sup>	mapping ~ 3° × 3° field centered on M31

<sup>a</sup>Not new discoveries, but studies on the objects found by Hubble (1932) and Seyfert & Nassau (1945).

<sup>b</sup>With 254 class A, 99 class B, 152 class C, and 218 class D objects, where class A objects are very high-confidence objects, class B objects are high confidence objects, class C objects are plausible candidates, and class D miscellaneous non-stellar objects with an expected percentage of actual clusters of the order of a few percent.

<sup>c</sup>With 12 reliable, 4 possible.

<sup>d</sup>With 3 class A, 1 class B, 20 class C, and 20 class D objects.

<sup>e</sup>With 2 class A, 2 class B, 28 class C, and 36 class D objects.

<sup>f</sup>Observations of 13 fields centered on M31, but no GC search. Of the 435 objects, 268 have optical photometry in four or more filters, 224 have near-infrared photometry, 200 have radial velocities, and 188 have spectroscopic metallicities.

<sup>g</sup>Spectroscopy for 288 previously known objects. They presented a spectroscopic database of 321 velocities and 301 metallicities.

<sup>h</sup>2MASS near-infrared photometry for 693 known and candidate GCs. Of 1035 objects, 337 are confirmed GCs, 688 are GC candidates, and 10 are objects with controversial classification.

<sup>i</sup>Confirmed GC nature from spectroscopy of 76 candidates.

<sup>j</sup>With 113 class 1, 258 class 2, and 234 class 3, where classes 1, 2, and 3 are similar to classes A, B, and C, respectively, in Battistini et al. (1987).

Crampton, D., Cowley, A. P., Schade, D., & Chayer, P. 1985, *ApJ*, 288, 494  
 De Angeli, F., Piotto, G., Cassisi, S., Busso, G., Recio-Blanco, A., Salaris, M., Aparicio, A., & Rosenberg, A. 2005, *AJ*, 130, 116  
 Galleti, S., Federici, L., Bellazzini, M., Fusi Pecci, F., & Macrina, S. 2004, *A&A*, 416, 917  
 Galleti, S., Federici, L., Bellazzini, M., Buzzoni, A., & Fusi Pecci, F. 2006, *A&A*, 456, 985  
 Geisler, D. 1996, *AJ*, 111, 480  
 Hubble, E. P. 1932, *ApJ*, 76, 44  
 Huchra, J. P., Brodie, J. P., & Kent, S. M. 1991, *ApJ*, 370, 495  
 Huxor, A. P., Tanvir, N. R., Irwin, M. J., Ibata, R., Collett, J. L., Ferguson, A. M. N., Bridges, T., & Lewis, G. F. 2005, *MNRAS*, 360, 1007  
 Karachentsev, I. D., Karachentseva, V. E., Huchtmeier, W. K., & Makarov, D. I. 2004, *AJ*, 127, 2031  
 Kim, S. C., Lee, M. G., Geisler, D., Seguel, J., Sarajedini, A., & Harris, W. E. 2002, in *IAU Symp. 207, Extragalactic Star Clusters*, ed. D. Geisler, E. K. Grebel, & D. Minniti, 143  
 Kodaira, K., Vansevicius, V., Bridzius, A., Komiyama, Y., Miyazaki, S., Stonkute, R., Sabelviciute, I., & Narbutis, D. 2004, *PASJ*, 56, 1025  
 Lee, M. G., Kim, S. C., Geisler, D., Seguel, J., Sarajedini, A., & Harris, W. E. 2002, in *IAU Symp. 207, Extragalactic Star Clusters*, ed. D. Geisler, E. K. Grebel, & D. Minniti, 46  
 Mackey, A. D., Huxor, A., Ferguson, A. M. N., Tanvir, N. R., Irwin, M., Ibata, R., Bridges, T., Johnson, R. A., & Lewis, G. 2006, *ApJ*, 653, L105  
 Mackey, A. D., Huxor, A., Ferguson, A. M. N., Tanvir, N. R., Irwin, M., Ibata, R., Bridges, T., Johnson, R. A., & Lewis, G. 2007, *ApJ*, 655, L85  
 Martin, N. F., Ibata, R. A., Irwin, M. J., Chapman, S., Lewis, G. F., Ferguson, A. M. N., Tanvir, N., & McConnachie, A. W. 2006, *MNRAS*, 371, 1983  
 Mayall, N. U., & Eggen, O. J. 1953, *PASP*, 65, 24

Mochejska, B. J., Kaluzny, J., Krockenberger, M., Sasselov, D. D., & Stanek, K. Z. 1998, *Acta Astronomica*, 48, 455  
 Morrison, H. L., Harding, P., Hurley-Keller, D., & Jacoby, G. 2003, *ApJ*, 596, L183  
 Perrett, K. M., Bridges, T. J., Hanes, D. A., Irwin, M. J., Brodie, J. P., Carter, D., Huchra, J. P., & Watson, F. G. 2002, *AJ*, 123, 2490  
 Racine, R. 1991, *AJ*, 101, 865  
 Salaris, M., & Weiss, A. 2002, *A&A*, 388, 492  
 Santos, J. F. C., Jr., Alloin, D., Bica, E., & Bonatto, C. 2002, in *Extragalactic Star Clusters*, *IAU Symp. 207*, eds. D. Geisler, E. K. Grebel, & D. Minniti, 727  
 Sarajedini, A., Bedin, L. R., Chaboyer, B., Dotter, A., Siegel, M., Anderson, J., Aparicio, A., King, I., Majewski, S., Marín-Franch, A., Piotto, G., Reid, I. N., & Rosenberg, A. 2007, *AJ*, accepted (astro-ph/0612598)  
 Sargent, W. L. W., Kowal, C. T., Hartwick, F. D. A., & van den Bergh, S. 1977, *AJ*, 82, 947  
 Seguel, J., Geisler, D., Lee, M. G., Kim, S. C., Sarajedini, A., & Harris, W. E. 2002, in *IAU Symp. 207, Extragalactic Star Clusters*, ed. D. Geisler, E. K. Grebel, & D. Minniti, 146  
 Seyfert, C. K., & Nassau, J. J. 1945, *ApJ*, 102, 377  
 Strom, K. M. 1977, *Standard Stars for IIDS Observations*, Kitt Peak National Observatory  
 Tonry, J. T., & Davis, M. 1979, *AJ*, 84, 1511  
 Valdes, F. 1995, *Guide to the HYDRA Reduction Task DOHYDRA*  
 van den Bergh, S., & Mackey, A. D. 2004, *MNRAS*, 354, 713  
 Vetešník, M. 1962, *Bull. Astr. Inst. Czech*, 13, 180  
 Wirth, A., Smarr, L. L., & Bruno, T. L. 1985, *ApJ*, 290, 140

TABLE 2  
SUMMARY OF KPNO 0.9 M PHOTOMETRIC OBSERVATIONS

Night	Obs. Date (UT)	Field	Weather
(1)	(2)	(3)	(4)
N1	1996 October 14	23(C) 26	cloudy
N2	1996 October 15	16 17 18(long) <sup>a</sup> 19 20 23( <i>M</i> , <i>T</i> <sub>1</sub> ) 24 25(long) <sup>b</sup> 27	cloudy
N3	1996 October 16	<b>18(short)<sup>a</sup> 25(short)<sup>b</sup> 30 31 32 33 34 35</b>	<b>semi-photometric</b>
N4	1996 October 17	<b>28 36</b>	<b>semi-photometric</b>
N5	1996 October 18	<b>09 10 37 38 39 40 41</b>	<b>photometric</b>
N6	1996 October 19	. . .	. . .
N7	1996 October 20	. . .	. . .
N8	1996 October 21	<b>11 12 13 14 15 29 42 43(<i>M</i>)</b>	<b>photometric</b>
N9	1996 October 22	<b>43(<i>C</i>, <i>T</i><sub>1</sub>) 44 45<sup>c</sup></b>	<b>photometric</b>
N10	1996 October 23	(45 <sup>c</sup> ) 46 47 48 49 50	non-photometric
N11	1996 October 24	<b>01 02 03 04 05</b>	<b>semi-photometric</b>
N12	1996 October 25	06	non-photometric
Oct98	1998 October 19	<b>07 08 21 22 51 52 56</b>	<b>photometric</b>

NOTE. — The fields with standard transformation data (photometric and semi-photometric nights) are represented with bold letters.

<sup>a</sup> For the field of F18, which is just the northern field of F25, we took two sets of data; long exposures (1500s in *C*, 600s in *M*, and 600s in *T*<sub>1</sub>) and short exposures (300s in *C*, 100s in *M*, and 100s  $\times$  2 in *T*<sub>1</sub>).

<sup>b</sup> For the field of F25, which includes the M31 central region, we took of data; long exposures (1500s in *C*, 600s in *M*, and 300s  $\times$  2 in *T*<sub>1</sub>) and short exposures (300s in *C*, 200s in *M*, and 200s  $\times$  2 in *T*<sub>1</sub>).

<sup>c</sup> Field 45 was observed both on N9 and N10 with the same exposure time setups. Even though the seeing of N10 for F45 was slightly better than that of N9 (1.''6 versus 2.''0), we primarily used the N9 data for the utilization of N9 standard transformation information.

TABLE 3  
SUMMARY OF WIYN 3.5 M SPECTROSCOPIC OBSERVATIONS

Obs. Date (UT)	Hydra Configuration	N(observed) <sup>a</sup> (=new <sup>b</sup> + old <sup>c</sup> )	N(vel) <sup>d</sup>	Exposure Time
2000 September 7	1	68 (= 66+ 2)	38	1800 s $\times$ 4 = 7200 s (2 <sup>h</sup> )
2000 September 7	2	73 (= 56+17)	66	1800 s $\times$ 3 + 900 s = 6300 s (1 <sup>h</sup> 45 <sup>m</sup> )
2000 September 8	3	64 (= 64+ 0)	47	1800 s $\times$ 4 = 7200 s (2 <sup>h</sup> )
2000 September 8	4	62 (= 59+ 3)	34	1800 s $\times$ 3 = 5400 s (1 <sup>h</sup> 30 <sup>m</sup> )
2000 September 8	5	71 (= 59+12)	56	1800 s $\times$ 4 = 7200 s (2 <sup>h</sup> )
2000 September 9	6	75 (= 74+ 1)	36	1800 s $\times$ 4 = 7200 s (2 <sup>h</sup> )
2000 September 9	B	70 (= 67+ 3)	56	1800 s $\times$ 4 = 7200 s (2 <sup>h</sup> )
2000 September 9	E	70 (= 60+10)	57	1800 s $\times$ 3 + 1041 s = 6441 s (1 <sup>h</sup> 47 <sup>m</sup> 21 <sup>s</sup> )
	sub-total	552 (=504+48)	390	
2001 November 2	11	69 (= 54+15)	35	2400 s $\times$ 3 = 7200 s (2 <sup>h</sup> )
2001 November 2	12	79 (= 45+34)	60	2400 s $\times$ 3 = 7200 s (2 <sup>h</sup> )
2001 November 2	17	47 (= 38+ 9)	20	2400 s $\times$ 1 = 2400 s (40 <sup>m</sup> )
	sub-total	195 (=137+58)	115	
	Total	748 (=642+106)	505	

<sup>a</sup>Number of all observed objects.

<sup>b</sup>GC candidates found from the photometric criteria in this study.

<sup>c</sup>Previously known GCs.

<sup>d</sup>Number of objects for which successful velocities were measured.

TABLE 4  
NUMBER OF GLOBULAR CLUSTERS FOUND IN THIS STUDY

Class	Previously found by others <sup>a</sup>	New GCs	Sum
1	383	113	496
2	109	258	367
3	67	234	301
Sum	559	605	1164

<sup>a</sup>in Huxor et al. (2005); Galleti et al. (2006); Mackey et al. (2007) and references there in.

TABLE 5  
A LIST OF NEW GLOBULAR CLUSTERS (CLASS 1)

ID	R.A. <sup>a</sup> (J2000.0)	Dec <sup>b</sup> (J2000.0)	$T_1$	$(M - T_1)$	$(C - T_1)$	$v$ (km s <sup>-1</sup> )
(1)	(2)	(3)	(4)	(5)	(6)	(7)
1	00:36:33.54	+40:39:44.3	17.251 ± 0.007	0.650 ± 0.011	1.542 ± 0.015	-239.5 ± 46.7
2	00:36:34.99	+41:01:08.0	18.805 ± 0.030	0.677 ± 0.047	1.407 ± 0.060	-402.7 ± 92.5
3	00:37:10.67	+41:41:17.4	17.834 ± 0.011	0.778 ± 0.019	1.787 ± 0.030	-315.9 ± 34.5
4	00:38:01.31	+42:04:06.0	18.311 ± 0.016	0.708 ± 0.027	1.565 ± 0.040	-27.4 ± 32.8
5	00:38:59.15	+41:40:27.4	18.848 ± 0.031	0.877 ± 0.077	1.842 ± 0.083	-405.2 ± 43.1
6	00:39:39.69	+40:33:56.4	18.811 ± 0.045	0.648 ± 0.062	1.456 ± 0.078	-319.9 ± 53.5
7	00:39:44.03	+40:51:18.4	17.630 ± 0.017	0.204 ± 0.020	-0.068 ± 0.018	-390.4 ± 86.6
8	00:40:00.39	+40:43:53.5	18.581 ± 0.038	0.769 ± 0.057	1.628 ± 0.070	-108.9 ± 27.9
9	00:40:05.54	+40:56:14.0	19.374 ± 0.079	0.885 ± 0.125	1.464 ± 0.132	-422.7 ± 90.2
10	00:40:05.95	+40:35:38.9	18.154 ± 0.025	0.961 ± 0.040	1.365 ± 0.041	-585.0 ± 26.3
11	00:40:16.82	+40:39:33.7	18.697 ± 0.041	0.652 ± 0.056	1.817 ± 0.087	-581.5 ± 20.0
12	00:40:18.94	+41:00:50.9	18.125 ± 0.025	0.840 ± 0.039	1.897 ± 0.055	-429.9 ± 61.3
13	00:40:22.34	+40:50:07.5	18.568 ± 0.038	0.855 ± 0.059	1.831 ± 0.079	-104.5 ± 52.9
14	00:40:24.79	+40:48:46.4	17.460 ± 0.014	0.495 ± 0.019	0.989 ± 0.019	-495.0 ± 41.0
15	00:40:26.15	+40:45:31.9	19.716 ± 0.110	0.699 ± 0.158	0.808 ± 0.139	-542.5 ± 55.9
16	00:40:31.69	+40:46:08.1	19.259 ± 0.070	1.016 ± 0.119	2.319 ± 0.206	-675.6 ± 42.1
17	00:40:48.20	+41:00:32.2	18.867 ± 0.050	0.456 ± 0.066	0.964 ± 0.067	-510.6 ± 25.4
18	00:40:53.51	+41:16:14.7	18.701 ± 0.048	0.724 ± 0.063	1.274 ± 0.067	-285.8 ± 24.9
19	00:41:04.95	+41:28:37.8	18.225 ± 0.029	1.058 ± 0.043	2.450 ± 0.078	-137.7 ± 41.9
20	00:41:13.34	+41:09:41.6	19.614 ± 0.112	0.698 ± 0.145	0.285 ± 0.122	-513.0 ± 73.2
21	00:41:14.89	+40:49:38.2	18.251 ± 0.040	0.939 ± 0.060	1.711 ± 0.067	-222.6 ± 39.1
22	00:41:15.87	+40:28:28.7	18.631 ± 0.025	0.760 ± 0.040	1.329 ± 0.045	-343.0 ± 64.1
23	00:41:17.83	+40:43:34.5	18.976 ± 0.078	0.944 ± 0.118	1.239 ± 0.105	-548.7 ± 49.0
24	00:41:19.61	+40:39:29.2	18.987 ± 0.034	1.052 ± 0.065	2.857 ± 0.184	-465.9 ± 38.5
25	00:41:22.18	+40:49:57.5	19.321 ± 0.104	1.375 ± 0.202	2.889 ± 0.394	-625.0 ± 28.3
26	00:41:24.58	+40:36:03.2	18.904 ± 0.032	0.780 ± 0.052	2.036 ± 0.090	-568.0 ± 55.2
27	00:41:24.83	+40:45:19.4	19.167 ± 0.092	1.031 ± 0.146	1.726 ± 0.155	-498.8 ± 46.9
28	00:41:31.65	+40:59:28.7	18.832 ± 0.066	1.536 ± 0.144	2.733 ± 0.223	-408.2 ± 33.2
29	00:41:33.26	+40:39:38.6	18.718 ± 0.061	0.755 ± 0.085	1.377 ± 0.087	-537.5 ± 60.0
30	00:41:33.98	+40:42:22.2	18.882 ± 0.071	0.738 ± 0.098	1.646 ± 0.115	-476.3 ± 38.4
31	00:41:35.17	+40:53:41.1	19.530 ± 0.128	1.118 ± 0.213	1.649 ± 0.208	-519.3 ± 38.6
32	00:41:38.42	+40:58:26.0	18.749 ± 0.063	0.630 ± 0.083	1.491 ± 0.094	-448.0 ± 24.6
33	00:41:40.44	+40:46:08.9	19.017 ± 0.081	0.742 ± 0.112	1.145 ± 0.105	-501.4 ± 36.3
34	00:41:41.71	+40:52:00.9	18.571 ± 0.054	0.815 ± 0.077	1.051 ± 0.068	-531.8 ± 45.7
35	00:41:47.25	+41:52:34.0	19.310 ± 0.071	1.084 ± 0.157	3.183 ± 0.789	-385.2 ± 55.8
36	00:41:47.34	+40:51:07.5	18.871 ± 0.070	0.877 ± 0.102	1.977 ± 0.137	-419.2 ± 65.2
37	00:41:50.88	+40:45:12.9	19.896 ± 0.183	0.460 ± 0.228	0.516 ± 0.204	-364.4 ± 56.2
38	00:41:50.89	+40:52:47.1	17.720 ± 0.024	0.916 ± 0.037	1.675 ± 0.041	-383.0 ± 41.6
39	00:41:51.06	+41:20:14.8	18.114 ± 0.070	0.580 ± 0.093	1.135 ± 0.102	-246.1 ± 35.3
40	00:41:53.79	+40:54:48.4	18.802 ± 0.066	0.683 ± 0.089	1.478 ± 0.099	-464.5 ± 70.2
41	00:42:02.26	+40:53:45.5	18.910 ± 0.074	0.381 ± 0.090	0.705 ± 0.085	-453.7 ± 60.7
42	00:42:03.96	+40:56:51.2	19.614 ± 0.140	1.004 ± 0.220	0.765 ± 0.164	-536.7 ± 26.3
43	00:42:05.25	+40:48:01.5	18.493 ± 0.049	0.904 ± 0.074	1.780 ± 0.087	-297.0 ± 75.2
44	00:42:06.33	+40:53:15.6	18.328 ± 0.043	0.829 ± 0.062	1.138 ± 0.056	-490.5 ± 45.5
45	00:42:09.52	+40:47:43.5	15.497 ± 0.003	0.657 ± 0.005	1.449 ± 0.005	-543.8 ± 52.3
46	00:42:13.18	+40:46:11.5	18.975 ± 0.077	0.703 ± 0.106	1.289 ± 0.107	-416.6 ± 43.5
47	00:42:14.27	+40:50:07.0	19.681 ± 0.148	0.629 ± 0.197	1.184 ± 0.196	-434.9 ± 63.4
48	00:42:17.59	+40:55:15.3	18.129 ± 0.036	0.711 ± 0.049	1.216 ± 0.048	-409.4 ± 42.9
49	00:42:19.45	+40:52:21.7	19.378 ± 0.112	0.822 ± 0.160	1.541 ± 0.172	-373.5 ± 65.9
50	00:42:21.54	+41:14:19.9	17.508 ± 0.040	0.891 ± 0.060	1.876 ± 0.087	-347.5 ± 43.1
51	00:42:32.10	+40:53:34.0	18.869 ± 0.069	1.206 ± 0.121	2.436 ± 0.186	-373.2 ± 34.6
52	00:42:37.31	+41:50:53.5	18.186 ± 0.027	0.591 ± 0.044	1.135 ± 0.058	-99.1 ± 25.2
53	00:42:40.78	+40:17:52.0	17.858 ± 0.013	0.784 ± 0.020	1.713 ± 0.028	-347.6 ± 25.9
54	00:42:45.05	+41:08:15.4	17.702 ± 0.048	0.759 ± 0.068	1.678 ± 0.092	-509.8 ± 25.0
55	00:42:51.82	+40:44:09.3	18.074 ± 0.034	0.787 ± 0.048	1.734 ± 0.058	-675.9 ± 76.0
56	00:42:54.27	+41:01:53.0	18.405 ± 0.046	0.606 ± 0.060	1.447 ± 0.068	-442.2 ± 47.1
57	00:42:58.06	+41:23:03.3	14.627 ± 0.003	0.514 ± 0.004	1.119 ± 0.005	-220.6 ± 19.7
58	00:43:05.93	+41:50:59.5	18.945 ± 0.054	0.648 ± 0.091	0.855 ± 0.099	-301.0 ± 54.3
59	00:43:09.87	+41:19:01.2	17.111 ± 0.027	1.059 ± 0.046	2.519 ± 0.096	-165.8 ± 35.3
60	00:43:11.84	+40:56:04.9	18.561 ± 0.052	1.070 ± 0.085	2.170 ± 0.117	-203.6 ± 68.7
61	00:43:13.62	+41:38:28.0	18.754 ± 0.075	0.151 ± 0.085	1.069 ± 0.090	-253.4 ± 41.5
62	00:43:14.46	+41:53:46.6	19.081 ± 0.060	0.588 ± 0.095	1.444 ± 0.155	-50.7 ± 27.6
63	00:43:16.02	+41:27:57.0	17.644 ± 0.026	1.036 ± 0.040	2.451 ± 0.062	-215.0 ± 40.5
64	00:43:18.28	+40:59:23.6	19.305 ± 0.051	0.536 ± 0.072	1.634 ± 0.108	-259.0 ± 42.7
65	00:43:20.01	+41:39:41.5	18.094 ± 0.041	0.655 ± 0.053	1.261 ± 0.052	-373.0 ± 110.5
66	00:43:24.18	+41:38:42.5	19.808 ± 0.198	0.838 ± 0.275	1.182 ± 0.244	-197.1 ± 25.6
67	00:43:27.53	+41:35:34.8	17.988 ± 0.036	1.023 ± 0.055	2.249 ± 0.074	-183.8 ± 42.2
68	00:43:28.10	+41:00:21.2	19.083 ± 0.041	0.783 ± 0.067	1.948 ± 0.109	-342.0 ± 104.5
69	00:43:34.31	+41:43:38.9	18.222 ± 0.046	0.937 ± 0.067	1.459 ± 0.062	-382.4 ± 64.9
70	00:43:39.75	+41:29:16.4	18.485 ± 0.057	0.976 ± 0.084	2.369 ± 0.126	-70.3 ± 46.8
71	00:43:46.52	+41:39:29.1	18.760 ± 0.073	1.017 ± 0.110	2.620 ± 0.192	-149.1 ± 27.6
72	00:43:46.61	+41:22:28.0	16.973 ± 0.012	0.835 ± 0.017	1.826 ± 0.020	-160.2 ± 38.7
73	00:43:48.49	+41:07:48.0	17.507 ± 0.019	0.897 ± 0.027	1.924 ± 0.033	-32.8 ± 40.8
74	00:43:50.26	+41:41:47.9	18.375 ± 0.053	0.823 ± 0.073	1.563 ± 0.075	-90.1 ± 33.8
75	00:43:52.45	+41:38:30.0	18.873 ± 0.083	0.892 ± 0.119	1.499 ± 0.114	-116.4 ± 39.2
76	00:43:52.93	+41:45:17.8	18.343 ± 0.051	0.923 ± 0.074	1.646 ± 0.075	-139.5 ± 39.1
77	00:43:56.29	+41:19:47.9	17.813 ± 0.025	0.633 ± 0.033	1.377 ± 0.034	-149.6 ± 55.6
78	00:43:58.53	+41:25:02.4	17.687 ± 0.028	0.821 ± 0.039	1.390 ± 0.038	-219.9 ± 38.6
79	00:44:04.58	+41:32:09.3	18.025 ± 0.038	1.154 ± 0.061	2.175 ± 0.073	-258.4 ± 25.9
80	00:44:06.81	+41:49:03.7	18.070 ± 0.024	0.361 ± 0.034	1.367 ± 0.058	-145.7 ± 22.1
81	00:44:07.02	+41:47:52.9	18.676 ± 0.041	1.043 ± 0.084	2.322 ± 0.207	-71.4 ± 29.8
82	00:44:07.32	+41:47:05.4	19.327 ± 0.075	0.599 ± 0.119	1.377 ± 0.186	-83.8 ± 39.1
83	00:44:09.96	+41:51:28.2	19.027 ± 0.056	1.240 ± 0.134	2.187 ± 0.257	-139.9 ± 23.6
84	00:44:12.28	+41:21:11.1	18.192 ± 0.036	0.791 ± 0.049	1.051 ± 0.044	-80.5 ± 61.7
85	00:44:20.70	+41:41:45.2	18.419 ± 0.056	0.772 ± 0.076	0.882 ± 0.064	-55.3 ± 34.5
86	00:44:26.03	+41:35:14.4	17.243 ± 0.018	0.895 ± 0.026	2.133 ± 0.035	-68.8 ± 23.2
87	00:44:27.35	+41:57:56.3	18.084 ± 0.024	0.805 ± 0.043	1.306 ± 0.057	-113.9 ± 25.7
88	00:44:31.84	+41:52:22.0	18.482 ± 0.033	1.070 ± 0.070	3.470 ± 0.439	-116.8 ± 90.4
89	00:44:35.89	+41:38:00.3	18.812 ± 0.077	1.009 ± 0.116	2.249 ± 0.158	-86.4 ± 18.5
90	00:44:42.60	+41:41:10.0	18.915 ± 0.087	0.718 ± 0.115	1.304 ± 0.111	-125.4 ± 30.5
91	00:44:46.84	+41:46:43.6	18.338 ± 0.030	1.215 ± 0.071	1.501 ± 0.082	-40.2 ± 25.0
92	00:44:51.53	+41:50:56.2	19.299 ± 0.074	0.500 ± 0.112	1.050 ± 0.146	-174.6 ± 25.5
93	00:44:58.44	+41:56:36.6	18.940 ± 0.053	0.928 ± 0.101	1.505 ± 0.142	-68.8 ± 44.4
94	00:44:59.30	+41:33:05.1	18.160 ± 0.043	0.774 ± 0.059	1.447 ± 0.059	-8.4 ± 28.9
95	00:45:02.20	+41:49:39.0	18.741 ± 0.044	1.118 ± 0.096	1.777 ± 0.145	-14.7 ± 42.4
96	00:45:02.21	+41:23:36.9	17.942 ± 0.029	0.625 ± 0.037	1.327 ± 0.038	-312.9 ± 51.6
97	00:45:05.17	+41:42:29.7	18.521 ± 0.061	0.599 ± 0.077	1.227 ± 0.076	-131.1 ± 21.2
98	00:45:07.59	+41:35:16.1	18.553 ± 0.062	0.837 ± 0.087	1.361 ± 0.081	-193.4 ± 59.3
99	00:45:08.19	+41:36:43.5	18.300 ± 0.030	0.617 ± 0.047	1.135 ± 0.062	-135.4 ± 54.5
100	00:45:13.91	+41:31:33.4	18.236 ± 0.046	0.894 ± 0.066	1.569 ± 0.066	-123.2 ± 57.6
101	00:45:18.25	+41:49:35.9	18.795 ± 0.045	0.880 ± 0.081	1.769 ± 0.132	-67.7 ± 46.4
102	00:45:39.85	+41:52:46.8	18.079 ± 0.024	0.597 ± 0.037	1.213 ± 0.047	-75.8 ± 47.2
103	00:45:40.80	+40:39:51.5	17.949 ± 0.011	0.714 ± 0.019	1.625 ± 0.028	-176.2 ± 28.1

TABLE 5 — *Continued*

ID (1)	R.A. <sup>a</sup> (J2000.0) (2)	Decl. <sup>b</sup> (J2000.0) (3)	$T_1$ (4)	$(M - T_1)$ (5)	$(C - T_1)$ (6)	$v$ (km s <sup>-1</sup> ) (7)
104	00:45:44.28	+41:57:27.4	17.367 ± 0.012	0.917 ± 0.023	1.741 ± 0.035	-301 ± 17.2
105	00:45:51.82	+41:57:41.2	18.497 ± 0.034	0.704 ± 0.056	1.500 ± 0.083	-128.5 ± 25.2
106	00:45:52.08	+42:05:26.0	18.939 ± 0.051	1.021 ± 0.101	1.829 ± 0.158	-889.9 ± 38.2
107	00:46:50.78	+41:42:27.5	18.055 ± 0.019	0.820 ± 0.029	1.801 ± 0.038	-21.2 ± 58.1
108	00:47:14.24	+40:38:12.3	15.657 ± 0.002	0.600 ± 0.003	1.107 ± 0.004	-396.5 ± 37.6
109	00:47:16.82	+41:03:11.3	18.852 ± 0.028	0.439 ± 0.041	1.287 ± 0.052	11.8 ± 55.4
110	00:47:55.75	+41:27:32.8	19.010 ± 0.038	0.663 ± 0.069	1.509 ± 0.109	-16.2 ± 58.6
111	00:48:14.58	+41:29:19.4	18.672 ± 0.027	0.841 ± 0.056	1.894 ± 0.107	-206.2 ± 40.7
112	00:48:15.87	+41:23:31.2	15.880 ± 0.002	0.495 ± 0.004	1.072 ± 0.004	-251.9 ± 46.3
113	00:48:40.23	+41:55:44.6	17.904 ± 0.015	0.640 ± 0.026	1.262 ± 0.037	-48.8 ± 22.4

NOTE. — Table 5 is published in its entirety in the electronic edition of the *Astronomical Journal*. A portion is shown here for guidance regarding its form and content.

<sup>a</sup> Right ascension in units of hours, minutes, and seconds.

<sup>b</sup> Declination in units of degrees, arcminutes, and arcseconds.

TABLE 6  
A LIST OF NEW PROBABLE GLOBULAR CLUSTERS (CLASS 2)

ID	R.A. <sup>a</sup> (J2000.0)	Dec. <sup>b</sup> (J2000.0)	$T_1$	$(M - T_1)$	$(C - T_1)$	$v$ (km s <sup>-1</sup> )
(1)	(2)	(3)	(4)	(5)	(6)	(7)
1	00:33:23.07	+40:04:40.7	17.784 ± 0.015	0.896 ± 0.036	2.223 ± 0.102	...
2	00:33:32.20	+39:51:32.8	17.534 ± 0.010	0.505 ± 0.014	1.009 ± 0.014	...
3	00:33:37.03	+39:40:59.0	16.283 ± 0.004	0.794 ± 0.006	1.570 ± 0.007	...
4	00:34:34.20	+40:02:49.4	18.777 ± 0.038	1.145 ± 0.106	2.277 ± 0.266	...
5	00:35:21.20	+41:55:32.6	17.957 ± 0.013	1.031 ± 0.025	2.646 ± 0.065	...
6	00:35:34.24	+41:11:53.0	18.409 ± 0.018	0.883 ± 0.033	1.826 ± 0.050	...
7	00:35:45.26	+39:39:21.3	18.334 ± 0.020	0.943 ± 0.036	2.435 ± 0.082	...
8	00:35:58.15	+39:37:35.5	17.527 ± 0.010	0.963 ± 0.018	1.938 ± 0.028	...
9	00:36:00.23	+40:56:19.2	18.624 ± 0.025	1.249 ± 0.055	2.728 ± 0.132	...
10	00:36:01.70	+39:48:50.2	17.916 ± 0.014	0.965 ± 0.025	2.316 ± 0.052	...
11	00:36:02.02	+41:14:43.4	18.930 ± 0.029	0.652 ± 0.047	1.144 ± 0.052	...
12	00:36:05.08	+40:55:19.6	17.252 ± 0.008	1.288 ± 0.017	2.343 ± 0.029	...
13	00:36:31.70	+41:11:41.3	18.042 ± 0.013	1.006 ± 0.026	2.192 ± 0.047	...
14	00:36:32.68	+40:37:46.5	19.045 ± 0.034	0.757 ± 0.054	1.673 ± 0.080	...
15	00:37:09.75	+40:11:36.0	16.105 ± 0.004	0.488 ± 0.007	1.051 ± 0.010	...
16	00:37:19.08	+40:47:48.3	17.802 ± 0.013	0.683 ± 0.020	1.368 ± 0.024	...
17	00:37:30.44	+40:36:43.8	17.535 ± 0.012	0.986 ± 0.021	2.450 ± 0.047	...
18	00:37:30.82	+40:18:23.9	18.493 ± 0.028	0.807 ± 0.046	1.640 ± 0.063	...
19	00:37:33.47	+40:05:28.7	18.213 ± 0.030	1.010 ± 0.066	2.180 ± 0.174	...
20	00:37:35.68	+40:35:14.4	18.256 ± 0.022	1.215 ± 0.047	2.625 ± 0.105	...
21	00:37:53.16	+41:31:09.3	18.904 ± 0.033	0.764 ± 0.075	1.602 ± 0.075	...
22	00:37:54.31	+40:17:26.7	17.886 ± 0.022	1.272 ± 0.059	2.530 ± 0.172	...
23	00:38:00.42	+41:34:15.6	18.583 ± 0.025	0.840 ± 0.060	1.462 ± 0.051	...
24	00:38:11.00	+40:38:51.4	18.650 ± 0.032	0.748 ± 0.051	1.933 ± 0.088	...
25	00:38:43.98	+40:24:58.9	19.373 ± 0.062	0.747 ± 0.099	1.226 ± 0.108	...
26	00:38:48.68	+40:31:18.3	18.541 ± 0.030	0.156 ± 0.037	-0.038 ± 0.033	...
27	00:39:09.20	+40:28:28.6	16.956 ± 0.007	0.652 ± 0.011	1.387 ± 0.014	...
28	00:39:13.65	+41:57:51.6	18.551 ± 0.024	0.555 ± 0.037	1.323 ± 0.049	...
29	00:39:23.80	+42:01:37.1	18.892 ± 0.033	0.623 ± 0.052	1.180 ± 0.061	...
30	00:39:27.03	+42:06:56.0	19.077 ± 0.039	0.521 ± 0.059	1.187 ± 0.072	...
31	00:39:42.04	+40:52:20.6	17.841 ± 0.020	0.359 ± 0.025	0.306 ± 0.023	...
32	00:39:44.93	+42:07:04.7	16.924 ± 0.006	0.653 ± 0.009	1.495 ± 0.013	...
33	00:39:46.32	+40:53:09.4	18.473 ± 0.035	0.608 ± 0.049	0.619 ± 0.043	...
34	00:39:51.16	+40:45:32.8	19.079 ± 0.061	0.501 ± 0.081	0.865 ± 0.079	...
35	00:39:58.93	+41:45:40.1	17.846 ± 0.013	0.897 ± 0.024	1.936 ± 0.039	...
36	00:40:00.01	+40:22:13.8	17.756 ± 0.018	0.856 ± 0.027	1.027 ± 0.025	...
37	00:40:00.35	+40:48:50.8	17.899 ± 0.021	0.663 ± 0.030	1.342 ± 0.033	...
38	00:40:03.64	+40:44:04.1	16.834 ± 0.008	0.697 ± 0.012	1.596 ± 0.015	...
39	00:40:05.00	+41:47:17.6	18.599 ± 0.025	0.683 ± 0.041	1.207 ± 0.048	...
40	00:40:07.53	+41:58:11.4	19.337 ± 0.050	0.546 ± 0.075	1.305 ± 0.098	...
41	00:40:10.27	+41:01:23.7	18.601 ± 0.045	0.496 ± 0.054	0.143 ± 0.048	...
42	00:40:13.96	+41:41:35.6	19.132 ± 0.066	1.079 ± 0.098	2.134 ± 0.144	...
43	00:40:15.32	+40:36:53.7	18.056 ± 0.023	0.384 ± 0.029	0.438 ± 0.027	...
44	00:40:18.78	+40:31:14.2	17.611 ± 0.015	0.985 ± 0.025	2.127 ± 0.040	...
45	00:40:19.30	+40:32:42.4	14.921 ± 0.002	1.351 ± 0.003	2.986 ± 0.007	...
46	00:40:25.04	+40:37:57.7	18.230 ± 0.027	0.775 ± 0.039	1.351 ± 0.043	...
47	00:40:28.99	+41:42:17.6	18.594 ± 0.041	0.818 ± 0.054	1.445 ± 0.060	...
48	00:40:30.94	+40:39:22.7	17.675 ± 0.016	0.744 ± 0.023	1.127 ± 0.024	...
49	00:40:32.34	+42:00:51.9	18.702 ± 0.028	0.662 ± 0.045	1.798 ± 0.077	...
50	00:40:35.20	+41:47:32.3	19.019 ± 0.037	0.866 ± 0.067	1.261 ± 0.072	...
51	00:40:35.93	+40:39:06.8	18.937 ± 0.053	0.458 ± 0.070	1.176 ± 0.078	...
52	00:40:37.95	+40:38:03.7	18.372 ± 0.030	0.786 ± 0.045	1.704 ± 0.060	...
53	00:40:42.91	+41:23:39.9	17.812 ± 0.022	0.560 ± 0.027	1.077 ± 0.028	...
54	00:40:51.39	+41:42:46.7	18.859 ± 0.051	1.754 ± 0.112	3.538 ± 0.327	...
55	00:40:52.60	+41:32:27.5	18.803 ± 0.049	0.492 ± 0.059	0.530 ± 0.056	...
56	00:40:54.75	+41:58:46.1	18.184 ± 0.017	1.176 ± 0.038	2.539 ± 0.085	...
57	00:40:55.72	+41:28:05.3	17.792 ± 0.020	0.955 ± 0.028	2.024 ± 0.040	...
58	00:40:56.49	+41:31:54.2	17.906 ± 0.022	0.693 ± 0.028	1.396 ± 0.032	...
59	00:40:57.18	+40:44:31.1	19.761 ± 0.114	0.153 ± 0.135	0.907 ± 0.149	...
60	00:40:57.47	+41:00:37.1	18.133 ± 0.026	0.475 ± 0.034	0.838 ± 0.033	...
61	00:40:57.92	+41:03:38.4	18.418 ± 0.038	0.289 ± 0.044	-0.013 ± 0.040	...
62	00:40:58.44	+41:07:51.3	18.907 ± 0.057	1.073 ± 0.086	2.108 ± 0.125	...
63	00:41:01.21	+41:44:29.5	17.768 ± 0.020	0.358 ± 0.023	0.447 ± 0.022	...
64	00:41:01.94	+41:08:21.3	18.756 ± 0.050	1.050 ± 0.075	1.832 ± 0.092	...
65	00:41:05.05	+41:11:06.1	18.433 ± 0.038	0.805 ± 0.050	1.562 ± 0.060	...
66	00:41:05.57	+42:12:55.4	18.115 ± 0.034	0.918 ± 0.076	2.321 ± 0.232	...
67	00:41:05.59	+41:07:42.2	17.731 ± 0.020	0.855 ± 0.028	1.278 ± 0.028	...
68	00:41:06.38	+41:09:36.8	18.497 ± 0.041	0.300 ± 0.047	0.378 ± 0.045	...
69	00:41:07.53	+42:02:47.8	18.514 ± 0.024	0.740 ± 0.040	1.300 ± 0.047	...
70	00:41:08.90	+41:09:55.3	16.965 ± 0.010	1.013 ± 0.015	2.094 ± 0.022	...
71	00:41:10.87	+40:23:06.0	18.030 ± 0.022	0.764 ± 0.032	1.453 ± 0.038	...
72	00:41:12.12	+41:36:10.2	18.257 ± 0.030	0.635 ± 0.038	1.041 ± 0.038	...
73	00:41:12.31	+42:14:26.5	17.944 ± 0.029	1.278 ± 0.084	3.236 ± 0.422	...
74	00:41:12.67	+41:39:37.6	18.582 ± 0.040	0.573 ± 0.050	0.957 ± 0.050	...
75	00:41:14.68	+41:08:44.4	17.217 ± 0.031	0.201 ± 0.037	0.016 ± 0.034	...
76	00:41:17.66	+40:52:25.0	19.032 ± 0.081	0.793 ± 0.115	1.798 ± 0.143	...
77	00:41:19.15	+40:45:03.3	17.889 ± 0.028	0.848 ± 0.041	1.887 ± 0.053	...
78	00:41:25.37	+40:30:52.6	19.018 ± 0.036	1.084 ± 0.069	0.653 ± 0.047	...
79	00:41:26.91	+40:47:06.3	19.251 ± 0.100	0.890 ± 0.148	1.410 ± 0.145	...
80	00:41:26.97	+40:41:36.0	17.940 ± 0.030	0.498 ± 0.038	0.751 ± 0.036	...
81	00:41:37.35	+40:59:18.2	15.199 ± 0.003	0.552 ± 0.004	1.147 ± 0.004	...
82	00:41:38.55	+40:52:32.6	16.985 ± 0.013	0.438 ± 0.016	0.743 ± 0.015	...
83	00:41:38.65	+40:43:58.3	17.515 ± 0.021	0.732 ± 0.029	0.557 ± 0.023	...
84	00:41:40.12	+40:50:05.7	19.874 ± 0.177	0.488 ± 0.224	1.079 ± 0.226	...
85	00:41:40.62	+40:58:17.9	17.888 ± 0.028	0.863 ± 0.041	2.067 ± 0.059	...
86	00:41:42.63	+40:53:22.5	18.706 ± 0.061	0.609 ± 0.080	1.181 ± 0.080	...
87	00:41:48.22	+40:47:31.5	18.396 ± 0.045	0.788 ± 0.064	1.502 ± 0.069	...
88	00:41:51.48	+40:47:06.6	16.614 ± 0.009	0.699 ± 0.013	1.236 ± 0.013	...
89	00:41:54.70	+40:47:14.6	18.102 ± 0.035	1.373 ± 0.067	1.632 ± 0.056	...
90	00:41:56.93	+40:29:41.7	18.807 ± 0.029	1.035 ± 0.055	2.044 ± 0.083	...
91	00:41:59.90	+40:46:03.5	16.441 ± 0.008	0.559 ± 0.010	1.023 ± 0.010	...
92	00:42:03.77	+40:47:35.9	18.064 ± 0.033	1.064 ± 0.054	1.945 ± 0.064	...
93	00:42:06.55	+40:52:01.3	20.020 ± 0.199	0.985 ± 0.310	2.137 ± 0.435	...
94	00:42:07.81	+41:01:10.0	17.523 ± 0.020	0.975 ± 0.031	2.183 ± 0.046	...
95	00:42:14.58	+40:51:11.5	17.502 ± 0.021	0.435 ± 0.026	0.220 ± 0.022	...
96	00:42:16.53	+41:24:46.6	19.916 ± 0.042	1.177 ± 0.086	1.913 ± 0.130	...
97	00:42:16.76	+41:24:16.5	19.253 ± 0.024	0.578 ± 0.035	1.074 ± 0.042	...
98	00:42:16.83	+40:51:42.7	18.018 ± 0.032	0.750 ± 0.045	1.809 ± 0.057	...
99	00:42:19.55	+41:27:02.9	19.279 ± 0.024	0.532 ± 0.035	1.042 ± 0.042	...
100	00:42:20.30	+40:51:22.5	17.913 ± 0.030	0.448 ± 0.037	0.536 ± 0.034	...
101	00:42:21.51	+41:27:59.2	19.127 ± 0.021	0.596 ± 0.032	1.051 ± 0.037	...
102	00:42:22.65	+40:22:22.9	17.947 ± 0.014	0.915 ± 0.024	2.174 ± 0.042	...
103	00:42:24.06	+41:37:33.6	17.288 ± 0.005	0.592 ± 0.007	0.979 ± 0.008	...



TABLE 6 — *Continued*

ID	R.A. <sup>a</sup> (J2000.0)	Decl. <sup>b</sup> (J2000.0)	$T_1$ (4)	$(M - T_1)$ (5)	$(C - T_1)$ (6)	$v$ (km s <sup>-1</sup> ) (7)
(1)	(2)	(3)	(4)	(5)	(6)	(7)
104	00:42:24.94	+40:36:29.1	21.860 ± 0.481	0.609 ± 0.709	1.239 ± 0.808	...
105	00:42:25.06	+41:21:14.1	17.047 ± 0.026	0.664 ± 0.036	1.459 ± 0.045	...
106	00:42:28.17	+40:51:36.1	17.252 ± 0.016	0.624 ± 0.022	1.279 ± 0.023	...
107	00:42:33.12	+41:10:52.0	17.443 ± 0.038	0.822 ± 0.055	1.647 ± 0.072	...
108	00:42:35.14	+40:33:28.0	19.055 ± 0.037	1.028 ± 0.068	1.496 ± 0.072	...
109	00:42:35.15	+40:52:22.7	17.543 ± 0.021	0.783 ± 0.030	1.543 ± 0.032	...
110	00:42:35.17	+41:30:18.1	19.497 ± 0.030	0.192 ± 0.038	-0.087 ± 0.035	...
111	00:42:39.05	+41:16:58.5	16.531 ± 0.016	0.896 ± 0.025	1.525 ± 0.030	...
112	00:42:46.36	+41:18:33.0	17.744 ± 0.050	0.826 ± 0.073	1.303 ± 0.078	...
113	00:42:55.13	+40:59:44.7	18.221 ± 0.039	0.604 ± 0.052	0.717 ± 0.046	...
114	00:42:56.07	+40:59:54.1	17.782 ± 0.026	0.374 ± 0.032	0.631 ± 0.030	...
115	00:42:56.47	+40:41:07.3	18.909 ± 0.072	1.379 ± 0.140	2.132 ± 0.156	...
116	00:42:56.78	+40:30:11.8	18.847 ± 0.030	0.897 ± 0.052	2.217 ± 0.098	...
117	00:42:59.93	+41:14:44.2	16.105 ± 0.011	0.590 ± 0.015	1.257 ± 0.018	...
118	00:43:00.00	+41:20:44.0	16.788 ± 0.021	0.787 ± 0.030	1.674 ± 0.041	...
119	00:43:05.70	+41:15:58.7	16.610 ± 0.018	0.506 ± 0.023	0.880 ± 0.024	...
120	00:43:05.97	+41:23:08.1	18.876 ± 0.017	0.701 ± 0.027	1.564 ± 0.041	...
121	00:43:08.88	+41:25:54.6	17.917 ± 0.008	0.868 ± 0.013	1.829 ± 0.022	...
122	00:43:09.21	+40:38:11.0	18.822 ± 0.030	0.650 ± 0.045	1.290 ± 0.052	...
123	00:43:09.24	+41:34:01.2	19.005 ± 0.019	0.499 ± 0.028	0.668 ± 0.028	...
124	00:43:18.30	+42:02:03.3	17.949 ± 0.020	0.727 ± 0.036	1.885 ± 0.076	...
125	00:43:18.88	+42:15:11.1	14.978 ± 0.002	0.850 ± 0.004	1.965 ± 0.010	...
126	00:43:21.27	+41:19:21.6	18.000 ± 0.030	0.443 ± 0.037	1.012 ± 0.037	...
127	00:43:22.55	+41:45:37.8	18.422 ± 0.032	1.134 ± 0.072	2.065 ± 0.134	...
128	00:43:22.86	+42:01:42.4	18.311 ± 0.029	0.975 ± 0.058	2.115 ± 0.126	...
129	00:43:26.15	+41:18:07.5	18.258 ± 0.039	0.386 ± 0.046	0.610 ± 0.043	...
130	00:43:26.32	+41:53:00.3	19.631 ± 0.097	1.013 ± 0.198	2.200 ± 0.452	...
131	00:43:26.60	+42:16:19.7	18.487 ± 0.047	1.155 ± 0.123	2.736 ± 0.439	...
132	00:43:26.69	+41:40:41.7	19.071 ± 0.101	0.715 ± 0.133	1.122 ± 0.122	...
133	00:43:26.86	+40:25:00.7	19.313 ± 0.040	1.086 ± 0.082	1.811 ± 0.109	...
134	00:43:27.94	+40:35:59.3	18.485 ± 0.019	0.825 ± 0.033	1.702 ± 0.048	...
135	00:43:33.22	+41:34:05.9	17.561 ± 0.025	0.698 ± 0.033	1.427 ± 0.034	...
136	00:43:37.89	+41:45:40.2	17.486 ± 0.014	1.217 ± 0.032	2.667 ± 0.092	...
137	00:43:39.22	+41:10:19.0	17.934 ± 0.029	0.536 ± 0.036	0.471 ± 0.032	...
138	00:43:39.28	+41:10:08.7	15.872 ± 0.005	0.361 ± 0.006	0.514 ± 0.005	...
139	00:43:41.37	+41:48:47.5	18.313 ± 0.030	0.759 ± 0.052	1.227 ± 0.066	...
140	00:43:42.76	+40:58:57.0	18.859 ± 0.034	1.105 ± 0.066	1.789 ± 0.080	...
141	00:43:44.90	+41:45:59.7	19.146 ± 0.063	0.745 ± 0.109	1.722 ± 0.201	...
142	00:43:45.07	+41:12:27.0	18.073 ± 0.032	1.124 ± 0.051	1.778 ± 0.051	...
143	00:43:51.21	+41:46:49.0	17.639 ± 0.017	0.375 ± 0.024	0.263 ± 0.022	...
144	00:43:52.28	+41:42:39.4	17.947 ± 0.035	0.896 ± 0.051	1.775 ± 0.055	...
145	00:43:52.78	+41:47:41.7	18.815 ± 0.048	0.540 ± 0.074	0.838 ± 0.083	...
146	00:43:52.80	+41:49:49.9	17.951 ± 0.021	0.841 ± 0.038	1.988 ± 0.082	...
147	00:43:53.17	+40:19:57.9	18.432 ± 0.018	0.629 ± 0.029	1.172 ± 0.033	...
148	00:43:55.11	+41:29:08.3	17.431 ± 0.021	1.311 ± 0.038	3.034 ± 0.077	...
149	00:43:56.51	+41:44:51.2	19.344 ± 0.078	0.230 ± 0.104	0.856 ± 0.136	...
150	00:43:57.21	+41:45:33.3	17.879 ± 0.034	0.646 ± 0.044	1.069 ± 0.041	...
151	00:43:57.83	+41:35:19.9	17.479 ± 0.023	0.739 ± 0.031	1.698 ± 0.035	...
152	00:43:59.32	+40:48:03.0	18.442 ± 0.023	0.587 ± 0.034	0.909 ± 0.034	...
153	00:44:00.06	+41:48:33.5	17.270 ± 0.012	0.745 ± 0.020	1.848 ± 0.040	...
154	00:44:00.11	+41:51:32.9	18.474 ± 0.034	1.173 ± 0.078	1.885 ± 0.123	...
155	00:44:01.82	+41:15:01.1	17.709 ± 0.023	0.487 ± 0.029	0.744 ± 0.027	...
156	00:44:03.96	+41:37:40.4	19.228 ± 0.119	0.165 ± 0.134	0.449 ± 0.127	...
157	00:44:07.97	+41:47:01.9	17.425 ± 0.014	0.388 ± 0.020	0.542 ± 0.021	...
158	00:44:09.57	+41:33:58.9	18.126 ± 0.043	0.435 ± 0.052	0.539 ± 0.047	...
159	00:44:10.55	+41:17:59.1	17.186 ± 0.015	0.316 ± 0.018	0.547 ± 0.016	...
160	00:44:10.88	+41:32:03.6	16.546 ± 0.010	0.277 ± 0.012	-0.062 ± 0.011	...
161	00:44:12.19	+41:36:37.6	18.215 ± 0.045	0.841 ± 0.064	1.490 ± 0.062	...
162	00:44:12.31	+41:35:16.8	17.222 ± 0.019	0.351 ± 0.022	0.586 ± 0.021	...
163	00:44:12.54	+41:17:19.9	17.835 ± 0.026	0.391 ± 0.032	0.251 ± 0.028	...
164	00:44:19.59	+41:51:33.3	18.163 ± 0.026	0.668 ± 0.043	1.292 ± 0.060	...
165	00:44:20.00	+40:57:58.1	18.413 ± 0.023	0.630 ± 0.034	1.264 ± 0.039	...
166	00:44:25.08	+41:20:49.5	15.391 ± 0.003	0.368 ± 0.004	0.441 ± 0.004	...
167	00:44:25.12	+40:56:14.4	18.812 ± 0.032	1.169 ± 0.065	2.142 ± 0.098	...
168	00:44:26.27	+40:15:04.7	17.247 ± 0.009	0.677 ± 0.017	1.412 ± 0.027	...
169	00:44:26.61	+40:42:45.4	18.392 ± 0.022	1.225 ± 0.046	2.645 ± 0.098	...
170	00:44:27.23	+41:37:15.9	18.077 ± 0.040	0.618 ± 0.052	1.162 ± 0.050	...
171	00:44:28.46	+40:42:23.8	17.498 ± 0.010	1.040 ± 0.019	2.511 ± 0.040	...
172	00:44:28.95	+41:20:10.3	17.556 ± 0.021	0.312 ± 0.024	0.441 ± 0.023	...
173	00:44:30.88	+41:18:22.0	17.544 ± 0.020	0.834 ± 0.028	1.952 ± 0.035	...
174	00:44:34.16	+41:47:44.9	19.168 ± 0.064	1.014 ± 0.130	2.176 ± 0.290	...
175	00:44:35.20	+40:43:52.9	18.324 ± 0.021	0.996 ± 0.038	2.297 ± 0.071	...
176	00:44:36.71	+41:52:47.6	18.282 ± 0.029	0.596 ± 0.046	1.556 ± 0.081	...
177	00:44:38.88	+41:55:10.6	18.059 ± 0.023	1.179 ± 0.052	2.789 ± 0.171	...
178	00:44:42.83	+41:25:05.7	17.982 ± 0.035	1.242 ± 0.060	3.105 ± 0.135	...
179	00:44:42.89	+41:33:26.2	17.258 ± 0.019	0.701 ± 0.025	1.312 ± 0.025	...
180	00:44:47.36	+41:25:53.8	18.138 ± 0.043	1.038 ± 0.066	0.953 ± 0.050	...
181	00:44:48.64	+42:06:08.1	18.486 ± 0.034	1.206 ± 0.079	2.523 ± 0.204	...
182	00:44:48.85	+41:47:58.2	18.172 ± 0.026	0.598 ± 0.042	1.268 ± 0.060	...
183	00:44:54.31	+41:32:14.2	17.945 ± 0.036	0.704 ± 0.047	1.370 ± 0.047	...
184	00:44:54.69	+41:52:31.6	18.772 ± 0.046	0.756 ± 0.079	0.926 ± 0.084	...
185	00:44:56.48	+41:52:54.5	18.150 ± 0.025	0.874 ± 0.047	1.848 ± 0.089	...
186	00:44:56.90	+41:16:11.5	17.830 ± 0.026	0.708 ± 0.034	1.579 ± 0.038	...
187	00:44:58.08	+41:09:42.3	16.080 ± 0.006	0.599 ± 0.007	1.341 ± 0.008	...
188	00:44:59.25	+41:53:18.5	18.892 ± 0.051	0.780 ± 0.089	1.156 ± 0.108	...
189	00:44:59.29	+40:58:22.0	19.349 ± 0.053	0.628 ± 0.079	1.428 ± 0.099	...
190	00:45:01.60	+40:24:11.1	17.312 ± 0.007	1.077 ± 0.014	2.397 ± 0.028	...
191	00:45:02.45	+41:59:33.3	18.578 ± 0.038	0.675 ± 0.063	1.456 ± 0.099	...
192	00:45:03.80	+40:29:59.3	17.948 ± 0.012	0.677 ± 0.019	1.266 ± 0.023	...
193	00:45:04.12	+40:43:07.3	18.058 ± 0.016	0.806 ± 0.027	2.294 ± 0.055	...
194	00:45:04.74	+40:30:31.9	18.462 ± 0.019	0.506 ± 0.028	1.011 ± 0.031	...
195	00:45:05.78	+41:59:03.6	18.181 ± 0.026	0.817 ± 0.047	1.613 ± 0.077	...
196	00:45:05.86	+40:41:07.5	18.820 ± 0.033	0.618 ± 0.049	1.317 ± 0.058	...
197	00:45:07.53	+41:00:12.7	18.788 ± 0.032	0.723 ± 0.050	1.039 ± 0.049	...
198	00:45:10.50	+41:50:19.6	17.864 ± 0.020	0.604 ± 0.032	0.970 ± 0.038	...
199	00:45:24.67	+41:42:56.6	18.862 ± 0.040	0.506 ± 0.053	0.757 ± 0.050	...
200	00:45:26.73	+41:39:48.2	22.273 ± 0.976	-1.213 ± 0.993	-1.594 ± 0.981	...
201	00:45:26.75	+41:38:41.2	19.057 ± 0.048	0.361 ± 0.060	0.666 ± 0.058	...
202	00:45:28.38	+41:30:51.9	18.611 ± 0.031	1.097 ± 0.054	2.210 ± 0.082	...
203	00:45:30.09	+41:43:49.0	18.913 ± 0.042	0.285 ± 0.052	0.355 ± 0.048	...
204	00:45:30.57	+40:47:58.2	18.667 ± 0.024	0.939 ± 0.046	2.401 ± 0.104	...
205	00:45:33.25	+40:17:08.4	18.754 ± 0.023	0.706 ± 0.039	1.528 ± 0.053	...
206	00:45:36.90	+41:44:18.3	16.065 ± 0.003	0.819 ± 0.005	1.963 ± 0.008	...
207	00:45:39.14	+41:49:55.0	18.241 ± 0.027	0.847 ± 0.049	1.497 ± 0.066	...

-97.0 ± 51.9

TABLE 6 — *Continued*

ID	R.A. <sup>a</sup>	Decl. <sup>b</sup>	$T_1$	$(M - T_1)$	$(C - T_1)$	$v$
(1)	(J2000.0)	(J2000.0)	(4)	(5)	(6)	(7)
208	00:45:41.07	+41:55:08.2	18.090 ± 0.024	0.351 ± 0.034	0.326 ± 0.032	...
209	00:45:41.70	+41:51:42.6	17.951 ± 0.021	0.697 ± 0.035	0.960 ± 0.037	...
210	00:45:47.05	+40:45:18.1	17.597 ± 0.009	0.974 ± 0.018	2.405 ± 0.040	...
211	00:45:47.20	+41:39:32.4	19.244 ± 0.056	0.916 ± 0.089	1.273 ± 0.084	...
212	00:45:52.10	+41:31:49.9	18.728 ± 0.034	0.906 ± 0.054	1.958 ± 0.077	...
213	00:45:53.84	+41:41:11.3	18.572 ± 0.030	0.683 ± 0.043	1.531 ± 0.052	...
214	00:45:54.06	+39:56:46.8	18.086 ± 0.019	1.133 ± 0.049	2.431 ± 0.135	...
215	00:45:59.57	+41:51:15.0	18.883 ± 0.049	0.794 ± 0.084	1.516 ± 0.120	...
216	00:46:02.65	+41:44:52.8	19.057 ± 0.049	-0.051 ± 0.056	-0.533 ± 0.051	...
217	00:46:09.34	+41:29:04.3	18.874 ± 0.040	0.669 ± 0.056	1.393 ± 0.064	...
218	00:46:10.03	+40:55:13.3	17.843 ± 0.012	0.959 ± 0.022	2.276 ± 0.045	...
219	00:46:11.34	+41:38:49.5	19.013 ± 0.045	0.784 ± 0.067	1.482 ± 0.075	...
220	00:46:17.78	+41:44:43.5	19.185 ± 0.063	0.910 ± 0.117	2.236 ± 0.269	...
221	00:46:19.24	+40:23:42.0	19.792 ± 0.059	0.732 ± 0.100	1.721 ± 0.156	...
222	00:46:26.60	+41:38:38.3	19.049 ± 0.047	0.798 ± 0.070	1.502 ± 0.079	...
223	00:46:32.88	+40:06:36.5	16.998 ± 0.007	0.833 ± 0.015	1.948 ± 0.034	...
224	00:46:38.75	+41:59:31.1	17.482 ± 0.014	0.776 ± 0.023	1.685 ± 0.038	...
225	00:46:42.61	+41:58:35.4	18.466 ± 0.034	0.553 ± 0.052	0.634 ± 0.050	...
226	00:46:47.82	+42:01:56.3	19.566 ± 0.092	0.942 ± 0.173	1.366 ± 0.203	...
227	00:46:54.48	+42:00:47.4	18.305 ± 0.030	0.589 ± 0.046	0.585 ± 0.042	...
228	00:46:55.50	+42:20:50.1	17.471 ± 0.020	0.549 ± 0.034	0.470 ± 0.033	...
229	00:47:00.31	+40:45:27.8	17.421 ± 0.008	0.719 ± 0.014	1.556 ± 0.019	...
230	00:47:02.15	+41:10:55.4	18.549 ± 0.021	0.895 ± 0.039	2.071 ± 0.066	...
231	00:47:14.11	+40:22:23.2	18.645 ± 0.021	0.507 ± 0.032	0.827 ± 0.033	...
232	00:47:14.43	+40:25:38.8	17.995 ± 0.012	0.930 ± 0.023	2.175 ± 0.043	...
233	00:47:15.19	+41:01:12.1	18.311 ± 0.017	0.706 ± 0.028	1.579 ± 0.038	...
234	00:47:35.21	+41:01:31.3	18.301 ± 0.019	0.518 ± 0.027	1.225 ± 0.033	...
235	00:47:54.06	+41:33:23.9	17.084 ± 0.007	0.612 ± 0.012	1.217 ± 0.016	...
236	00:47:57.88	+41:34:32.3	17.671 ± 0.012	0.634 ± 0.021	1.149 ± 0.025	...
237	00:47:58.40	+41:31:25.5	18.473 ± 0.023	0.685 ± 0.043	1.286 ± 0.058	...
238	00:48:01.66	+41:49:56.9	18.184 ± 0.019	0.542 ± 0.032	0.979 ± 0.040	...
239	00:48:09.68	+41:48:36.7	17.535 ± 0.011	0.584 ± 0.018	1.128 ± 0.024	...
240	00:48:24.14	+40:06:43.1	18.844 ± 0.039	0.922 ± 0.057	1.693 ± 0.155	...
241	00:48:24.77	+41:52:54.0	18.544 ± 0.027	0.646 ± 0.048	0.316 ± 0.039	...
242	00:48:26.60	+41:19:47.3	19.217 ± 0.042	1.081 ± 0.081	2.110 ± 0.133	...
243	00:48:27.19	+42:02:43.5	16.623 ± 0.005	1.011 ± 0.010	2.510 ± 0.030	...
244	00:48:27.39	+41:06:17.2	19.078 ± 0.036	1.036 ± 0.069	2.954 ± 0.226	...
245	00:48:30.38	+41:52:49.6	14.455 ± 0.001	1.000 ± 0.002	2.399 ± 0.004	...
246	00:48:30.63	+41:55:29.0	17.941 ± 0.015	1.083 ± 0.035	2.129 ± 0.073	...
247	00:48:32.16	+41:47:27.7	17.860 ± 0.014	0.574 ± 0.024	1.219 ± 0.035	...
248	00:48:32.71	+41:35:36.8	16.517 ± 0.004	0.864 ± 0.009	2.079 ± 0.018	...
249	00:48:32.96	+42:02:45.0	17.854 ± 0.014	0.928 ± 0.029	2.543 ± 0.094	...
250	00:48:36.64	+41:39:08.3	16.735 ± 0.005	0.527 ± 0.009	1.048 ± 0.011	...
251	00:48:40.67	+41:51:54.7	17.977 ± 0.016	0.494 ± 0.026	1.063 ± 0.035	...
252	00:48:41.13	+41:31:54.6	18.053 ± 0.016	0.731 ± 0.030	1.562 ± 0.047	...
253	00:48:42.18	+41:34:08.7	16.029 ± 0.003	0.580 ± 0.005	1.139 ± 0.006	...
254	00:48:50.01	+41:57:07.2	16.966 ± 0.006	0.862 ± 0.013	2.028 ± 0.028	...
255	00:49:02.95	+41:54:57.1	17.258 ± 0.008	0.812 ± 0.016	1.639 ± 0.027	...
256	00:49:05.38	+41:57:38.3	18.135 ± 0.017	1.096 ± 0.042	2.650 ± 0.132	...
257	00:49:15.21	+41:01:29.4	18.331 ± 0.019	0.544 ± 0.028	1.201 ± 0.033	...
258	00:50:17.46	+42:06:42.6	18.584 ± 0.026	0.910 ± 0.045	1.949 ± 0.074	...

NOTE. — Table 6 is published in its entirety in the electronic edition of the *Astronomical Journal*. A portion is shown here for guidance regarding its form and content.

<sup>a</sup> Right ascension in units of hours, minutes, and seconds.

<sup>b</sup> Declination in units of degrees, arcminutes, and arcseconds.

TABLE 7  
A LIST OF NEW POSSIBLE GLOBULAR CLUSTERS (CLASS 3)

ID	R.A. <sup>a</sup> (J2000.0)	Decl. <sup>b</sup> (J2000.0)	$T_1$	$(M - T_1)$	$(C - T_1)$	$v$ (km s <sup>-1</sup> )
(1)	(2)	(3)	(4)	(5)	(6)	(7)
1	00:33:13.08	+40:05:26.0	18.219 ± 0.023	0.990 ± 0.057	1.998 ± 0.127	...
2	00:33:15.82	+40:00:24.7	18.018 ± 0.019	0.968 ± 0.046	2.502 ± 0.159	...
3	00:33:34.43	+40:11:06.5	17.231 ± 0.009	0.897 ± 0.022	2.013 ± 0.052	...
4	00:33:34.96	+40:08:16.3	18.523 ± 0.030	1.166 ± 0.087	1.233 ± 0.093	...
5	00:33:38.04	+39:35:35.7	18.067 ± 0.015	1.182 ± 0.032	2.798 ± 0.069	...
6	00:33:46.11	+39:48:36.6	18.163 ± 0.017	0.990 ± 0.031	2.217 ± 0.049	...
7	00:33:54.63	+39:34:36.6	17.644 ± 0.010	1.311 ± 0.024	2.909 ± 0.052	...
8	00:34:11.50	+40:07:58.0	18.381 ± 0.026	0.974 ± 0.065	2.007 ± 0.148	...
9	00:34:12.20	+40:06:29.7	17.535 ± 0.012	1.092 ± 0.033	2.645 ± 0.115	...
10	00:34:26.85	+39:54:05.6	18.149 ± 0.017	0.773 ± 0.027	2.152 ± 0.046	...
11	00:34:51.16	+39:55:33.1	18.542 ± 0.030	0.946 ± 0.074	2.395 ± 0.236	...
12	00:35:08.81	+40:07:32.6	18.861 ± 0.041	0.983 ± 0.102	1.905 ± 0.213	...
13	00:35:09.24	+40:05:39.8	18.541 ± 0.030	1.000 ± 0.077	2.098 ± 0.185	...
14	00:35:14.86	+39:41:40.0	18.042 ± 0.015	1.039 ± 0.029	2.505 ± 0.067	...
15	00:35:20.47	+39:35:04.1	17.803 ± 0.012	1.089 ± 0.024	2.775 ± 0.066	...
16	00:35:22.00	+41:49:47.4	18.164 ± 0.016	1.136 ± 0.032	2.702 ± 0.082	...
17	00:35:28.44	+39:32:25.1	18.662 ± 0.027	0.866 ± 0.046	2.359 ± 0.104	...
18	00:35:29.32	+41:42:33.3	17.875 ± 0.011	1.172 ± 0.024	2.691 ± 0.060	...
19	00:35:29.68	+40:29:31.2	16.037 ± 0.003	0.581 ± 0.004	1.279 ± 0.005	...
20	00:35:49.74	+41:50:02.4	19.016 ± 0.034	1.107 ± 0.068	2.527 ± 0.154	...
21	00:35:50.83	+39:36:00.8	18.017 ± 0.015	1.037 ± 0.029	2.428 ± 0.061	...
22	00:35:51.76	+40:54:11.6	17.748 ± 0.012	1.316 ± 0.026	3.052 ± 0.077	...
23	00:35:53.10	+41:51:23.7	19.151 ± 0.038	1.597 ± 0.106	3.020 ± 0.258	...
24	00:35:53.83	+41:43:42.6	18.553 ± 0.020	0.729 ± 0.034	1.997 ± 0.065	...
25	00:35:54.22	+41:46:53.8	17.919 ± 0.013	1.181 ± 0.027	2.705 ± 0.066	...
26	00:36:05.61	+39:58:04.9	18.530 ± 0.035	0.903 ± 0.083	2.021 ± 0.193	...
27	00:36:12.50	+40:52:37.7	18.387 ± 0.021	1.055 ± 0.040	2.192 ± 0.070	...
28	00:36:16.95	+41:25:36.4	18.455 ± 0.019	0.950 ± 0.035	2.086 ± 0.063	...
29	00:36:22.26	+39:52:04.5	18.251 ± 0.018	1.215 ± 0.039	2.884 ± 0.108	...
30	00:36:27.36	+41:35:14.0	19.949 ± 0.072	1.022 ± 0.143	1.427 ± 0.154	...
31	00:36:31.43	+42:06:24.6	19.098 ± 0.037	0.738 ± 0.059	1.943 ± 0.107	...
32	00:36:33.36	+41:30:03.1	19.115 ± 0.033	1.071 ± 0.068	2.381 ± 0.144	...
33	00:36:37.89	+42:14:46.2	17.190 ± 0.007	1.189 ± 0.015	2.763 ± 0.038	...
34	00:36:43.42	+39:34:56.2	17.512 ± 0.010	0.991 ± 0.018	2.695 ± 0.048	...
35	00:36:46.66	+41:26:23.9	19.028 ± 0.031	1.071 ± 0.063	2.460 ± 0.141	...
36	00:36:47.20	+40:04:09.5	18.534 ± 0.035	0.985 ± 0.088	2.574 ± 0.304	...
37	00:36:49.19	+39:39:43.7	17.662 ± 0.011	1.109 ± 0.022	2.870 ± 0.063	...
38	00:36:52.96	+39:38:41.4	16.798 ± 0.005	1.188 ± 0.011	2.826 ± 0.028	...
39	00:37:00.98	+39:33:27.6	18.810 ± 0.030	1.317 ± 0.069	2.931 ± 0.187	...
40	00:37:03.40	+41:33:22.1	19.086 ± 0.032	1.150 ± 0.070	2.786 ± 0.192	...
41	00:37:05.08	+40:01:06.3	18.256 ± 0.028	0.927 ± 0.067	1.746 ± 0.121	...
42	00:37:06.28	+41:44:48.5	17.551 ± 0.009	0.930 ± 0.017	2.290 ± 0.035	...
43	00:37:09.10	+39:49:10.4	18.801 ± 0.030	0.921 ± 0.054	2.298 ± 0.113	...
44	00:37:10.58	+40:19:50.5	16.793 ± 0.005	1.250 ± 0.010	2.989 ± 0.029	...
45	00:37:12.95	+41:26:36.2	18.682 ± 0.023	0.723 ± 0.038	1.272 ± 0.045	...
46	00:37:28.93	+41:55:01.9	18.857 ± 0.026	1.153 ± 0.058	2.649 ± 0.151	...
47	00:37:33.49	+40:37:28.5	18.636 ± 0.032	0.621 ± 0.048	1.271 ± 0.057	...
48	00:37:37.20	+40:05:39.6	17.246 ± 0.012	0.978 ± 0.027	2.549 ± 0.097	...
49	00:37:37.27	+41:54:04.4	18.819 ± 0.025	1.620 ± 0.078	3.464 ± 0.285	...
50	00:37:41.27	+40:04:42.9	18.389 ± 0.035	1.113 ± 0.083	3.191 ± 0.474	...
51	00:37:41.79	+40:05:18.0	18.414 ± 0.036	0.979 ± 0.078	2.581 ± 0.292	...
52	00:37:58.06	+41:23:36.5	19.484 ± 0.066	1.974 ± 0.247	1.256 ± 0.123	-143.9 ± 39.7
53	00:38:00.76	+42:02:56.9	18.337 ± 0.016	1.136 ± 0.036	2.578 ± 0.089	...
54	00:38:06.10	+40:24:30.2	17.557 ± 0.012	0.846 ± 0.020	1.996 ± 0.035	...
55	00:38:12.84	+41:52:47.3	19.389 ± 0.042	1.574 ± 0.128	2.137 ± 0.162	...
56	00:38:22.50	+40:50:56.4	18.235 ± 0.019	1.001 ± 0.034	2.227 ± 0.062	...
57	00:38:43.47	+41:58:38.1	19.165 ± 0.034	1.209 ± 0.080	2.336 ± 0.155	...
58	00:38:48.40	+40:03:01.2	18.488 ± 0.038	0.762 ± 0.072	2.130 ± 0.215	...
59	00:38:53.72	+40:38:29.5	18.196 ± 0.022	0.327 ± 0.029	0.132 ± 0.025	...
60	00:38:53.92	+40:38:39.6	18.952 ± 0.042	0.819 ± 0.070	1.522 ± 0.088	-88.6 ± 79.7
61	00:38:59.20	+41:43:58.8	18.950 ± 0.034	0.943 ± 0.089	1.641 ± 0.080	...
62	00:39:01.20	+42:03:54.3	18.387 ± 0.017	1.084 ± 0.037	0.982 ± 0.030	...
63	00:39:07.46	+40:40:12.5	18.324 ± 0.021	0.622 ± 0.031	0.628 ± 0.028	...
64	00:39:09.71	+41:35:15.5	18.189 ± 0.017	0.160 ± 0.027	1.989 ± 0.051	...
65	00:39:10.65	+41:01:18.5	18.110 ± 0.017	0.667 ± 0.026	1.188 ± 0.029	...
66	00:39:15.19	+42:22:50.7	18.214 ± 0.038	0.748 ± 0.076	1.588 ± 0.142	...
67	00:39:19.80	+40:37:59.1	17.517 ± 0.014	1.155 ± 0.025	2.515 ± 0.049	...
68	00:39:23.43	+40:14:39.8	16.804 ± 0.013	0.598 ± 0.019	1.176 ± 0.037	...
69	00:39:28.39	+42:02:56.0	18.267 ± 0.019	1.143 ± 0.040	2.677 ± 0.102	...
70	00:39:38.84	+41:34:38.7	17.139 ± 0.011	1.033 ± 0.016	2.259 ± 0.026	...
71	00:39:57.70	+41:00:57.3	18.038 ± 0.026	1.068 ± 0.039	2.577 ± 0.079	...
72	00:39:59.08	+40:28:16.3	18.097 ± 0.024	0.229 ± 0.029	-0.062 ± 0.026	...
73	00:40:04.30	+40:14:10.7	17.928 ± 0.035	1.390 ± 0.082	2.469 ± 0.292	...
74	00:40:05.27	+41:26:36.0	18.896 ± 0.053	0.769 ± 0.070	1.422 ± 0.078	...
75	00:40:06.83	+41:43:09.2	18.896 ± 0.054	0.780 ± 0.070	1.267 ± 0.073	...
76	00:40:08.41	+40:37:58.6	18.159 ± 0.025	0.555 ± 0.034	0.751 ± 0.032	...
77	00:40:15.38	+41:54:23.7	18.740 ± 0.029	0.869 ± 0.053	0.285 ± 0.036	-131.9 ± 103.9
78	00:40:15.48	+40:46:23.1	19.087 ± 0.061	0.676 ± 0.088	1.027 ± 0.084	...
79	00:40:16.57	+41:34:04.9	18.706 ± 0.045	0.602 ± 0.056	0.996 ± 0.057	...
80	00:40:20.08	+41:55:07.0	18.267 ± 0.019	1.450 ± 0.050	3.220 ± 0.159	...
81	00:40:20.83	+41:38:43.9	17.184 ± 0.012	0.863 ± 0.016	2.017 ± 0.024	...
82	00:40:26.99	+41:33:18.5	18.999 ± 0.059	0.772 ± 0.077	1.396 ± 0.085	...
83	00:40:27.56	+41:23:14.5	18.773 ± 0.048	0.910 ± 0.066	1.987 ± 0.094	...
84	00:40:28.38	+41:39:06.8	18.467 ± 0.036	1.299 ± 0.060	1.907 ± 0.068	...
85	00:40:33.17	+40:51:53.8	17.817 ± 0.019	0.905 ± 0.031	2.044 ± 0.046	...
86	00:40:43.43	+41:35:34.2	18.739 ± 0.046	0.807 ± 0.061	1.542 ± 0.072	...
87	00:40:46.31	+41:41:01.9	18.240 ± 0.030	0.983 ± 0.042	1.836 ± 0.054	...
88	00:40:48.03	+40:40:40.1	19.227 ± 0.069	0.561 ± 0.094	1.808 ± 0.141	...
89	00:40:51.04	+40:16:45.8	16.966 ± 0.015	0.703 ± 0.023	1.367 ± 0.050	...
90	00:40:53.06	+40:00:43.3	18.617 ± 0.066	1.130 ± 0.129	3.031 ± 0.880	...
91	00:40:57.27	+40:21:54.8	17.519 ± 0.014	0.942 ± 0.022	2.159 ± 0.038	...
92	00:41:02.52	+40:48:15.5	17.792 ± 0.019	1.018 ± 0.032	2.325 ± 0.054	...
93	00:41:03.43	+40:46:06.3	18.213 ± 0.027	0.582 ± 0.038	1.392 ± 0.045	...
94	00:41:07.66	+41:33:41.3	18.750 ± 0.047	0.610 ± 0.058	1.004 ± 0.059	...
95	00:41:07.80	+41:51:32.6	19.304 ± 0.048	0.721 ± 0.080	1.471 ± 0.106	...
96	00:41:21.99	+42:08:26.2	18.136 ± 0.035	0.695 ± 0.067	1.397 ± 0.110	...
97	00:41:24.43	+42:20:14.1	17.395 ± 0.017	0.934 ± 0.039	2.348 ± 0.118	...
98	00:41:30.88	+40:39:07.5	19.144 ± 0.089	0.753 ± 0.124	2.083 ± 0.188	...
99	00:41:39.70	+40:56:32.5	18.147 ± 0.035	1.153 ± 0.060	2.671 ± 0.114	...
100	00:41:40.98	+41:04:05.8	17.635 ± 0.045	0.895 ± 0.068	2.073 ± 0.112	...
101	00:41:49.62	+41:55:25.9	16.184 ± 0.004	0.430 ± 0.007	1.187 ± 0.010	-90.1 ± 26.9
102	00:41:55.92	+40:50:19.7	14.800 ± 0.002	0.678 ± 0.003	1.432 ± 0.003	...
103	00:42:01.69	+40:47:43.5	18.233 ± 0.039	0.780 ± 0.055	1.607 ± 0.062	...

TABLE 7 — *Continued*

ID	R.A. <sup>a</sup>	Decl. <sup>b</sup>	$T_1$	$(M-T_1)$	$(C-T_1)$	$v$
(1)	(J2000.0)	(J2000.0)	(4)	(5)	(6)	(km s <sup>-1</sup> )
104	00:42:03.04	+40:43:48.8	18.399 ± 0.055	0.740 ± 0.085	1.813 ± 0.184	...
105	00:42:07.12	+41:55:48.3	18.367 ± 0.031	0.872 ± 0.059	1.960 ± 0.124	1.3 ± 24.9
106	00:42:08.45	+40:58:03.9	17.740 ± 0.025	0.632 ± 0.034	0.562 ± 0.029	...
107	00:42:14.18	+41:34:26.3	19.206 ± 0.023	0.672 ± 0.035	1.515 ± 0.053	...
108	00:42:23.35	+40:38:35.5	18.819 ± 0.030	1.450 ± 0.073	1.947 ± 0.079	...
109	00:42:30.05	+41:23:26.1	17.449 ± 0.038	0.736 ± 0.054	1.287 ± 0.060	...
110	00:42:33.09	+40:04:53.6	18.399 ± 0.055	1.289 ± 0.118	2.319 ± 0.274	...
111	00:42:41.72	+40:16:45.0	18.769 ± 0.028	0.784 ± 0.046	1.342 ± 0.051	...
112	00:42:44.53	+40:54:28.4	16.688 ± 0.009	1.214 ± 0.017	2.629 ± 0.029	...
113	00:42:45.16	+41:17:51.5	17.216 ± 0.031	0.907 ± 0.047	1.664 ± 0.059	...
114	00:42:48.13	+40:18:24.1	18.371 ± 0.020	0.746 ± 0.031	1.882 ± 0.050	...
115	00:42:49.80	+41:22:36.9	15.499 ± 0.007	0.535 ± 0.009	1.145 ± 0.011	...
116	00:42:51.20	+41:23:16.4	17.207 ± 0.030	0.542 ± 0.040	1.480 ± 0.053	...
117	00:43:01.16	+40:44:58.6	18.998 ± 0.078	1.094 ± 0.127	2.424 ± 0.207	...
118	00:43:05.24	+41:14:28.9	17.635 ± 0.044	1.015 ± 0.072	2.260 ± 0.128	...
119	00:43:08.93	+41:07:32.2	16.717 ± 0.019	1.524 ± 0.042	3.132 ± 0.108	...
120	00:43:10.21	+41:17:21.1	17.407 ± 0.036	0.995 ± 0.058	2.394 ± 0.115	...
121	00:43:15.09	+41:47:25.4	18.775 ± 0.045	1.093 ± 0.097	1.869 ± 0.160	-65.4 ± 48.8
122	00:43:15.94	+41:30:33.0	17.910 ± 0.033	1.402 ± 0.062	3.069 ± 0.123	...
123	00:43:21.38	+40:23:55.3	17.266 ± 0.007	0.991 ± 0.013	2.486 ± 0.029	...
124	00:43:23.90	+41:35:15.9	18.660 ± 0.068	0.947 ± 0.100	1.612 ± 0.098	...
125	00:43:27.11	+41:07:54.1	17.796 ± 0.025	0.861 ± 0.036	1.138 ± 0.031	...
126	00:43:30.00	+40:17:06.2	18.850 ± 0.026	0.541 ± 0.040	0.991 ± 0.043	...
127	00:43:34.36	+41:40:46.2	17.716 ± 0.028	1.182 ± 0.046	2.515 ± 0.069	...
128	00:43:41.87	+40:24:01.3	19.042 ± 0.031	0.849 ± 0.056	1.238 ± 0.058	...
129	00:43:42.74	+41:46:29.5	17.961 ± 0.021	0.758 ± 0.037	1.884 ± 0.076	...
130	00:43:44.36	+41:47:05.0	18.355 ± 0.032	0.166 ± 0.042	0.041 ± 0.040	...
131	00:43:45.22	+41:27:56.3	...	...	...	...
132	00:43:47.17	+41:27:44.9	17.431 ± 0.021	1.991 ± 0.061	3.355 ± 0.099	...
133	00:43:51.72	+40:37:43.2	18.736 ± 0.024	1.062 ± 0.048	2.231 ± 0.088	...
134	00:43:52.32	+41:36:22.8	18.686 ± 0.069	1.110 ± 0.109	2.172 ± 0.134	...
135	00:44:01.14	+41:04:05.6	17.824 ± 0.025	1.353 ± 0.045	3.087 ± 0.096	...
136	00:44:04.43	+40:05:19.6	18.417 ± 0.025	0.704 ± 0.049	1.540 ± 0.086	...
137	00:44:05.67	+41:15:51.7	18.045 ± 0.031	1.406 ± 0.057	2.958 ± 0.107	...
138	00:44:11.96	+42:11:06.7	17.678 ± 0.022	1.110 ± 0.056	2.898 ± 0.238	...
139	00:44:15.54	+41:53:32.0	18.449 ± 0.033	0.879 ± 0.062	1.898 ± 0.121	...
140	00:44:16.61	+40:36:26.3	19.223 ± 0.037	1.038 ± 0.073	2.078 ± 0.122	...
141	00:44:17.35	+41:49:16.7	17.617 ± 0.016	0.765 ± 0.027	1.635 ± 0.047	...
142	00:44:24.52	+41:51:45.5	17.811 ± 0.018	1.474 ± 0.051	3.021 ± 0.164	...
143	00:44:27.00	+41:38:34.4	17.963 ± 0.035	1.380 ± 0.065	2.706 ± 0.098	...
144	00:44:29.69	+41:55:36.3	18.330 ± 0.031	0.549 ± 0.047	1.115 ± 0.063	...
145	00:44:30.20	+41:54:48.8	19.113 ± 0.062	0.962 ± 0.121	1.590 ± 0.177	...
146	00:44:31.36	+41:36:49.2	16.326 ± 0.008	0.982 ± 0.012	2.180 ± 0.016	...
147	00:44:32.30	+40:16:39.9	17.990 ± 0.012	1.269 ± 0.028	2.655 ± 0.063	...
148	00:44:32.48	+40:38:56.3	17.291 ± 0.007	1.082 ± 0.014	2.603 ± 0.032	...
149	00:44:34.37	+41:51:18.3	20.502 ± 0.223	1.033 ± 0.463	1.017 ± 0.433	-212.3 ± 62.5
150	00:44:36.54	+41:46:46.6	17.863 ± 0.020	0.726 ± 0.034	1.501 ± 0.053	...
151	00:44:37.49	+42:08:49.5	18.140 ± 0.034	1.409 ± 0.108	3.284 ± 0.501	...
152	00:44:37.88	+41:51:53.4	17.990 ± 0.022	1.142 ± 0.050	1.219 ± 0.049	...
153	00:44:38.46	+41:25:11.4	16.057 ± 0.007	0.918 ± 0.010	1.021 ± 0.008	...
154	00:44:40.69	+41:56:46.3	18.370 ± 0.032	0.493 ± 0.047	1.261 ± 0.071	...
155	00:44:43.52	+41:47:20.1	18.128 ± 0.024	1.375 ± 0.064	2.960 ± 0.209	...
156	00:44:45.88	+40:35:19.6	19.162 ± 0.035	1.316 ± 0.084	2.407 ± 0.149	...
157	00:44:46.28	+40:33:06.8	19.644 ± 0.054	0.727 ± 0.090	1.426 ± 0.113	...
158	00:44:49.97	+40:23:15.4	18.249 ± 0.015	1.280 ± 0.036	2.601 ± 0.076	...
159	00:44:53.41	+41:31:56.4	19.577 ± 0.154	0.886 ± 0.219	2.600 ± 0.401	-63.5 ± 47.9
160	00:44:54.43	+40:06:44.1	18.307 ± 0.022	1.026 ± 0.054	2.486 ± 0.163	...
161	00:44:56.64	+41:54:58.7	18.274 ± 0.028	0.958 ± 0.055	2.169 ± 0.127	...
162	00:45:06.74	+40:44:07.4	18.227 ± 0.019	0.939 ± 0.033	2.501 ± 0.076	...
163	00:45:06.97	+42:17:47.2	18.452 ± 0.046	0.604 ± 0.083	1.837 ± 0.205	...
164	00:45:07.13	+41:23:46.8	18.661 ± 0.068	0.943 ± 0.099	1.934 ± 0.115	...
165	00:45:11.00	+40:35:14.7	18.801 ± 0.025	1.045 ± 0.050	2.196 ± 0.091	...
166	00:45:13.83	+41:42:34.8	19.119 ± 0.105	0.851 ± 0.147	1.344 ± 0.136	...
167	00:45:13.89	+41:42:26.9	18.177 ± 0.045	0.418 ± 0.054	0.560 ± 0.049	...
168	00:45:14.87	+41:40:12.5	18.836 ± 0.039	0.403 ± 0.050	0.907 ± 0.051	...
169	00:45:15.27	+41:47:40.2	17.693 ± 0.017	0.671 ± 0.027	1.149 ± 0.032	...
170	00:45:16.19	+41:43:22.8	20.173 ± 0.286	-0.009 ± 0.315	-0.043 ± 0.295	...
171	00:45:16.62	+41:41:02.1	19.104 ± 0.093	1.320 ± 0.168	1.443 ± 0.126	...
172	00:45:19.38	+41:22:51.8	18.472 ± 0.027	1.167 ± 0.049	2.721 ± 0.105	...
173	00:45:19.55	+41:36:10.9	18.421 ± 0.026	1.054 ± 0.045	1.815 ± 0.053	...
174	00:45:21.09	+41:30:01.7	19.152 ± 0.051	0.877 ± 0.079	1.570 ± 0.090	...
175	00:45:21.12	+41:40:56.1	18.938 ± 0.043	0.486 ± 0.056	0.649 ± 0.052	...
176	00:45:22.62	+42:19:18.3	16.236 ± 0.006	1.426 ± 0.020	3.229 ± 0.084	...
177	00:45:22.92	+41:30:17.5	18.519 ± 0.028	0.811 ± 0.043	2.102 ± 0.070	...
178	00:45:24.48	+41:27:41.4	18.135 ± 0.019	1.309 ± 0.039	3.125 ± 0.106	...
179	00:45:25.33	+40:19:00.3	18.853 ± 0.025	0.700 ± 0.042	1.328 ± 0.051	...
180	00:45:26.88	+41:15:45.0	19.111 ± 0.035	0.928 ± 0.066	1.834 ± 0.093	...
181	00:45:27.18	+41:41:59.1	19.025 ± 0.045	0.695 ± 0.065	1.446 ± 0.075	...
182	00:45:27.26	+41:32:54.0	18.427 ± 0.026	1.217 ± 0.049	2.524 ± 0.087	...
183	00:45:27.50	+41:23:23.8	17.197 ± 0.009	0.953 ± 0.014	2.356 ± 0.026	...
184	00:45:30.32	+41:37:13.7	17.962 ± 0.018	0.704 ± 0.025	1.372 ± 0.028	...
185	00:45:31.70	+41:28:31.7	18.744 ± 0.034	1.074 ± 0.060	2.366 ± 0.103	...
186	00:45:33.96	+41:28:06.6	19.163 ± 0.050	1.428 ± 0.109	2.900 ± 0.227	...
187	00:45:37.70	+41:54:04.0	18.508 ± 0.035	0.722 ± 0.058	1.184 ± 0.069	...
188	00:45:38.72	+41:53:41.0	19.047 ± 0.057	0.717 ± 0.094	1.397 ± 0.129	...
189	00:45:40.35	+41:42:15.8	18.662 ± 0.033	0.488 ± 0.044	1.038 ± 0.045	...
190	00:45:43.93	+41:54:26.6	17.427 ± 0.013	1.218 ± 0.029	2.343 ± 0.059	...
191	00:45:44.13	+41:42:53.7	17.604 ± 0.013	0.370 ± 0.017	0.335 ± 0.015	...
192	00:45:47.73	+41:52:17.0	19.374 ± 0.078	0.434 ± 0.112	0.679 ± 0.117	...
193	00:45:49.97	+40:05:09.1	16.678 ± 0.005	0.888 ± 0.012	2.306 ± 0.034	...
194	00:45:50.08	+41:43:49.9	18.313 ± 0.023	1.223 ± 0.043	3.432 ± 0.159	...
195	00:45:51.33	+40:25:45.1	17.890 ± 0.011	1.208 ± 0.024	2.682 ± 0.058	...
196	00:45:51.58	+40:04:43.8	18.188 ± 0.020	1.042 ± 0.051	2.094 ± 0.113	...
197	00:45:57.63	+40:17:09.5	17.843 ± 0.015	0.723 ± 0.030	1.590 ± 0.056	...
198	00:46:02.82	+40:23:04.0	18.905 ± 0.026	1.055 ± 0.054	2.712 ± 0.149	...
199	00:46:03.73	+41:36:29.2	18.885 ± 0.040	0.642 ± 0.056	1.392 ± 0.064	...
200	00:46:06.09	+40:22:26.0	17.497 ± 0.008	1.061 ± 0.016	2.469 ± 0.035	...
201	00:46:17.08	+41:36:35.7	18.442 ± 0.026	1.141 ± 0.047	2.757 ± 0.105	...
202	00:46:18.28	+41:47:01.1	18.860 ± 0.047	0.967 ± 0.091	2.033 ± 0.171	...
203	00:46:22.78	+40:57:48.8	18.454 ± 0.020	1.077 ± 0.041	2.602 ± 0.101	...
204	00:46:22.92	+40:20:42.2	18.660 ± 0.021	0.926 ± 0.040	2.286 ± 0.085	...
205	00:46:24.79	+40:35:08.4	17.657 ± 0.009	1.078 ± 0.018	2.610 ± 0.045	...
206	00:46:34.67	+40:30:40.9	19.004 ± 0.029	0.659 ± 0.047	1.632 ± 0.072	...
207	00:46:36.50	+41:10:31.9	18.684 ± 0.024	0.777 ± 0.041	1.602 ± 0.054	...

TABLE 7 — *Continued*

ID	R.A. <sup>a</sup> (J2000.0)	Decl. <sup>b</sup> (J2000.0)	$T_1$	$(M-T_1)$	$(C-T_1)$	$v$ (km s <sup>-1</sup> )
(1)	(2)	(3)	(4)	(5)	(6)	(7)
208	00:46:36.82	+40:43:01.4	18.386 ± 0.019	1.020 ± 0.038	2.229 ± 0.071	...
209	00:46:39.66	+41:51:35.5	19.192 ± 0.064	0.852 ± 0.114	2.200 ± 0.264	...
210	00:46:48.19	+41:45:40.2	17.934 ± 0.018	0.232 ± 0.022	0.190 ± 0.020	...
211	00:46:49.72	+41:45:44.6	17.759 ± 0.014	0.717 ± 0.021	1.667 ± 0.027	...
212	00:46:53.10	+41:22:07.2	18.149 ± 0.015	1.044 ± 0.030	2.588 ± 0.068	...
213	00:46:58.77	+42:17:45.3	18.491 ± 0.050	0.819 ± 0.102	1.120 ± 0.126	...
214	00:46:58.88	+40:54:02.6	17.472 ± 0.008	1.061 ± 0.017	2.597 ± 0.041	...
215	00:47:02.28	+41:03:25.0	18.734 ± 0.025	1.033 ± 0.049	2.481 ± 0.107	...
216	00:47:03.73	+41:39:14.5	18.343 ± 0.024	0.983 ± 0.040	2.627 ± 0.087	...
217	00:47:07.55	+41:41:18.7	18.583 ± 0.030	0.846 ± 0.047	1.701 ± 0.058	...
218	00:47:21.95	+42:26:57.6	17.982 ± 0.031	1.080 ± 0.077	2.158 ± 0.179	...
219	00:47:25.25	+41:02:21.0	18.835 ± 0.030	0.786 ± 0.049	1.377 ± 0.057	-86.8 ± 35.6
220	00:47:28.75	+41:53:49.7	17.024 ± 0.007	0.577 ± 0.012	1.385 ± 0.018	...
221	00:47:58.79	+41:39:33.4	19.014 ± 0.038	0.826 ± 0.076	1.796 ± 0.136	...
222	00:47:59.48	+41:54:13.0	19.077 ± 0.042	0.481 ± 0.069	1.280 ± 0.109	-3.4 ± 44.6
223	00:48:04.61	+40:08:27.0	17.289 ± 0.009	1.239 ± 0.017	2.381 ± 0.064	...
224	00:48:08.61	+41:49:08.1	17.564 ± 0.010	0.974 ± 0.023	2.501 ± 0.070	...
225	00:48:31.34	+42:01:05.5	17.027 ± 0.007	0.997 ± 0.015	2.490 ± 0.042	...
226	00:48:34.26	+41:54:26.8	17.292 ± 0.008	0.820 ± 0.017	2.103 ± 0.040	...
227	00:48:44.05	+42:15:48.8	18.500 ± 0.049	1.008 ± 0.116	3.014 ± 0.582	...
228	00:48:46.49	+41:46:45.8	19.456 ± 0.059	0.985 ± 0.132	1.643 ± 0.201	...
229	00:49:11.04	+41:57:53.1	19.548 ± 0.065	0.831 ± 0.132	1.104 ± 0.149	...
230	00:49:13.31	+41:01:01.4	15.286 ± 0.002	0.513 ± 0.002	1.186 ± 0.003	...
231	00:49:14.80	+41:09:08.2	17.503 ± 0.009	0.914 ± 0.016	2.330 ± 0.034	...
232	00:49:25.63	+42:06:06.7	17.943 ± 0.015	0.886 ± 0.025	2.253 ± 0.052	...
233	00:49:35.65	+42:11:42.8	18.278 ± 0.020	0.916 ± 0.034	2.663 ± 0.096	...
234	00:51:08.70	+42:11:27.0	16.686 ± 0.005	0.654 ± 0.008	1.390 ± 0.010	...

NOTE. — Table 7 is published in its entirety in the electronic edition of the *Astronomical Journal*. A portion is shown here for guidance regarding its form and content.

<sup>a</sup> Right ascension in units of hours, minutes, and seconds.

<sup>b</sup> Declination in units of degrees, arcminutes, and arcseconds.



TABLE 8  
A LIST OF STARS IDENTIFIED IN THIS STUDY

ID	R.A. <sup>a</sup> (J2000.0)	Decl. <sup>b</sup> (J2000.0)	$T_1$	$(M - T_1)$	$(C - T_1)$	$v$ (km s <sup>-1</sup> )
(1)	(2)	(3)	(4)	(5)	(6)	(7)
1	00:35:10.78	+41:44:03.1	16.340 ± 0.003	0.711 ± 0.005	1.701 ± 0.008	-15.9 ± 37.2
2	00:35:17.16	+41:22:13.0	16.014 ± 0.003	0.707 ± 0.004	1.669 ± 0.006	-54.5 ± 28.2
3	00:35:20.08	+41:21:41.7	15.935 ± 0.002	0.590 ± 0.004	1.341 ± 0.005	-1.0 ± 27.0
4	00:35:25.19	+42:06:51.3	16.863 ± 0.006	0.627 ± 0.009	1.344 ± 0.011	-102.1 ± 38.0
5	00:35:26.09	+41:44:42.0	15.639 ± 0.002	0.618 ± 0.003	1.421 ± 0.004	-66.8 ± 26.1
6	00:35:33.58	+42:07:06.8	14.486 ± 0.001	0.728 ± 0.002	1.730 ± 0.003	-38.7 ± 24.0
7	00:35:37.69	+42:07:03.5	15.766 ± 0.002	0.732 ± 0.004	1.707 ± 0.006	40.9 ± 43.1
8	00:35:45.46	+41:45:14.0	15.431 ± 0.002	0.581 ± 0.003	1.366 ± 0.004	-33.3 ± 24.7
9	00:36:08.99	+41:01:22.7	15.724 ± 0.002	0.554 ± 0.003	1.195 ± 0.004	-48.6 ± 28.7
10	00:36:21.26	+41:44:34.3	16.826 ± 0.005	0.674 ± 0.008	1.534 ± 0.011	-15.2 ± 23.3
11	00:36:27.38	+41:43:32.8	17.931 ± 0.012	1.236 ± 0.026	2.748 ± 0.065	-200.7 ± 64.9
12	00:36:30.70	+40:37:09.6	15.942 ± 0.002	0.663 ± 0.004	1.565 ± 0.005	26.2 ± 26.2
13	00:36:31.46	+41:01:09.0	14.533 ± 0.001	0.596 ± 0.002	1.385 ± 0.002	-97.2 ± 27.1
14	00:36:34.71	+41:42:45.6	14.219 ± 0.001	0.394 ± 0.001	0.919 ± 0.002	-11.9 ± 33.1
15	00:36:42.32	+41:45:15.5	18.025 ± 0.014	0.840 ± 0.024	1.987 ± 0.042	-24.4 ± 39.8
16	00:36:45.11	+41:00:48.1	15.943 ± 0.002	0.609 ± 0.004	1.326 ± 0.005	-65.1 ± 23.5
17	00:36:45.90	+41:42:38.2	15.724 ± 0.002	0.843 ± 0.004	2.073 ± 0.007	-10.6 ± 52.0
18	00:36:46.43	+41:20:53.4	14.513 ± 0.001	0.844 ± 0.002	2.078 ± 0.003	-53.8 ± 48.7
19	00:36:48.74	+42:06:11.9	15.744 ± 0.002	0.644 ± 0.004	1.571 ± 0.005	-62.3 ± 28.9
20	00:36:48.97	+41:42:29.0	16.144 ± 0.003	0.757 ± 0.005	1.795 ± 0.007	9.5 ± 32.8
21	00:36:57.44	+40:39:29.7	15.372 ± 0.002	0.778 ± 0.003	1.507 ± 0.004	-15.6 ± 24.0
22	00:37:00.12	+42:04:35.9	15.514 ± 0.002	0.618 ± 0.003	1.438 ± 0.004	-27.6 ± 28.0
23	00:37:03.70	+41:01:07.5	17.083 ± 0.006	0.563 ± 0.009	1.273 ± 0.011	-60.7 ± 26.2
24	00:37:04.69	+40:37:05.1	13.739 ± 0.001	0.491 ± 0.001	1.050 ± 0.001	-81.1 ± 27.8
25	00:37:05.54	+41:00:04.2	15.455 ± 0.002	0.781 ± 0.003	1.503 ± 0.004	-17.6 ± 24.9
26	00:37:05.79	+42:01:53.7	14.866 ± 0.001	0.522 ± 0.002	1.147 ± 0.002	-81.8 ± 31.3
27	00:37:06.13	+41:41:35.7	17.170 ± 0.006	0.474 ± 0.009	0.950 ± 0.011	-97.4 ± 55.7
28	00:37:08.27	+41:46:46.8	15.898 ± 0.002	0.577 ± 0.004	1.256 ± 0.005	48.8 ± 43.4
29	00:37:10.49	+40:34:04.5	16.751 ± 0.005	0.872 ± 0.008	2.166 ± 0.015	-50.8 ± 68.5
30	00:37:13.07	+40:17:10.0	15.544 ± 0.002	0.578 ± 0.003	1.358 ± 0.004	-54.7 ± 22.2
31	00:37:13.52	+41:38:58.5	16.776 ± 0.005	0.684 ± 0.011	1.525 ± 0.011	-105.8 ± 21.3
32	00:37:13.55	+41:57:47.7	14.940 ± 0.001	0.832 ± 0.002	2.148 ± 0.004	-50.0 ± 39.4
33	00:37:13.73	+41:42:23.9	14.681 ± 0.001	0.900 ± 0.003	2.065 ± 0.003	-2.8 ± 49.5
34	00:37:36.93	+41:00:21.0	15.424 ± 0.002	0.658 ± 0.003	1.294 ± 0.004	-20.7 ± 22.6
35	00:37:41.84	+41:00:43.4	16.006 ± 0.003	0.462 ± 0.005	0.988 ± 0.005	-91.2 ± 32.9
36	00:38:37.88	+41:23:18.9	17.326 ± 0.008	0.711 ± 0.018	1.534 ± 0.018	-131.0 ± 28.3
37	00:39:25.67	+41:45:20.5	16.062 ± 0.003	0.723 ± 0.005	1.722 ± 0.007	-49.8 ± 33.2
38	00:39:58.32	+40:39:22.0	15.887 ± 0.004	0.515 ± 0.005	1.020 ± 0.005	-77.2 ± 34.2
39	00:40:11.56	+41:51:46.1	18.051 ± 0.015	0.885 ± 0.028	2.139 ± 0.055	-77.1 ± 57.1
40	00:40:14.98	+41:00:47.0	17.351 ± 0.014	0.742 ± 0.019	1.623 ± 0.024	49.8 ± 34.9
41	00:40:16.27	+40:28:14.5	17.388 ± 0.013	0.833 ± 0.019	1.607 ± 0.024	-127.2 ± 50.6
42	00:40:17.63	+41:23:34.3	15.881 ± 0.004	0.603 ± 0.005	1.248 ± 0.006	-25.9 ± 29.2
43	00:40:18.08	+40:49:48.3	16.018 ± 0.004	0.679 ± 0.006	1.565 ± 0.007	-63.8 ± 32.8
44	00:40:24.24	+40:41:53.5	16.600 ± 0.007	0.618 ± 0.009	1.402 ± 0.011	-60.3 ± 27.4
45	00:40:24.96	+41:22:35.2	17.164 ± 0.012	0.878 ± 0.017	1.960 ± 0.024	-150.6 ± 51.9
46	00:40:32.79	+40:44:11.0	14.423 ± 0.001	0.834 ± 0.002	1.997 ± 0.003	-38.0 ± 60.0
47	00:40:35.32	+40:49:17.2	16.964 ± 0.009	0.698 ± 0.013	1.497 ± 0.016	-53.8 ± 33.7
48	00:40:39.37	+40:51:05.0	16.481 ± 0.006	0.612 ± 0.008	1.396 ± 0.010	-121.8 ± 25.8
49	00:40:43.20	+40:46:25.7	14.633 ± 0.001	0.594 ± 0.002	1.273 ± 0.002	-61.7 ± 35.1
50	00:40:47.35	+41:22:23.7	17.948 ± 0.024	0.710 ± 0.032	1.577 ± 0.039	-46.7 ± 23.5
51	00:41:02.59	+40:38:35.6	14.391 ± 0.001	0.523 ± 0.002	1.104 ± 0.002	-7.0 ± 43.4
52	00:41:02.76	+40:36:46.1	15.696 ± 0.003	0.720 ± 0.004	1.576 ± 0.006	-39.0 ± 31.7
53	00:41:03.35	+42:07:04.7	14.663 ± 0.002	0.456 ± 0.003	0.956 ± 0.004	-44.1 ± 39.0
54	00:41:07.13	+41:21:44.0	14.816 ± 0.002	0.601 ± 0.002	1.314 ± 0.003	-45.2 ± 27.7
55	00:41:09.47	+41:22:57.3	15.656 ± 0.004	0.813 ± 0.005	1.981 ± 0.007	-11.8 ± 58.0
56	00:41:09.80	+42:04:58.5	14.580 ± 0.001	0.552 ± 0.002	1.222 ± 0.002	-86.6 ± 22.6
57	00:41:09.92	+41:45:11.2	15.755 ± 0.002	0.505 ± 0.004	1.030 ± 0.004	-13.9 ± 32.8
58	00:41:10.48	+41:19:18.6	17.684 ± 0.019	0.725 ± 0.025	0.932 ± 0.024	-79.2 ± 21.0
59	00:41:11.20	+42:05:41.5	16.470 ± 0.004	0.530 ± 0.006	1.101 ± 0.007	-59.0 ± 33.3
60	00:41:12.00	+41:45:25.2	16.094 ± 0.003	0.474 ± 0.004	0.950 ± 0.005	-46.7 ± 26.8
61	00:41:13.87	+42:07:18.7	15.185 ± 0.002	0.509 ± 0.004	0.990 ± 0.006	-63.0 ± 33.4
62	00:41:14.76	+41:21:28.1	13.485 ± 0.001	0.618 ± 0.001	1.443 ± 0.001	-28.1 ± 21.7
63	00:41:20.93	+41:14:00.0	16.739 ± 0.020	0.560 ± 0.027	1.151 ± 0.030	-89.4 ± 44.2
64	00:41:21.80	+41:50:26.5	18.770 ± 0.046	0.378 ± 0.067	1.146 ± 0.100	46.4 ± 29.4
65	00:41:32.32	+42:04:35.2	16.262 ± 0.005	0.698 ± 0.008	1.936 ± 0.018	-137.8 ± 53.4
66	00:41:44.50	+41:45:31.7	13.545 ± 0.001	0.303 ± 0.001	0.892 ± 0.001	2.2 ± 24.5
67	00:41:54.46	+41:23:04.7	18.646 ± 0.014	0.852 ± 0.024	1.924 ± 0.043	-114.6 ± 77.0
68	00:42:01.51	+42:04:58.2	18.773 ± 0.045	0.905 ± 0.088	1.980 ± 0.184	10.6 ± 66.3
69	00:42:10.73	+41:46:39.4	19.099 ± 0.061	0.986 ± 0.126	1.811 ± 0.217	-31.0 ± 32.1
70	00:42:16.77	+40:25:47.1	16.565 ± 0.004	0.699 ± 0.007	1.601 ± 0.009	-119.4 ± 31.6
71	00:42:20.17	+42:06:54.4	15.148 ± 0.002	0.617 ± 0.004	1.393 ± 0.007	-20.1 ± 20.0
72	00:42:21.24	+41:22:47.2	19.717 ± 0.035	0.867 ± 0.060	1.447 ± 0.079	-6.5 ± 37.1
73	00:42:35.42	+41:45:08.9	14.414 ± 0.001	0.280 ± 0.002	0.813 ± 0.002	-29.5 ± 35.0
74	00:42:35.48	+42:03:42.0	18.861 ± 0.049	0.777 ± 0.088	1.809 ± 0.174	-104.6 ± 55.0
75	00:42:38.59	+42:07:07.0	16.255 ± 0.006	0.867 ± 0.013	2.195 ± 0.037	-96.9 ± 57.5
76	00:42:58.93	+42:06:06.9	16.468 ± 0.006	0.409 ± 0.009	1.180 ± 0.013	39.4 ± 22.7
77	00:43:00.52	+41:23:37.6	17.430 ± 0.005	0.474 ± 0.008	0.705 ± 0.008	-59.0 ± 34.4
78	00:43:00.86	+41:22:52.3	17.745 ± 0.007	0.735 ± 0.011	1.296 ± 0.014	-96.1 ± 25.2
79	00:43:06.04	+41:22:28.7	17.872 ± 0.054	1.371 ± 0.109	2.919 ± 0.261	-118.3 ± 58.1
80	00:43:06.92	+42:06:53.1	16.274 ± 0.006	0.835 ± 0.013	2.106 ± 0.035	-46.3 ± 51.2
81	00:43:08.86	+41:44:24.1	14.168 ± 0.001	0.452 ± 0.002	1.381 ± 0.002	-73.4 ± 23.1
82	00:43:10.86	+41:45:23.2	15.828 ± 0.003	0.267 ± 0.005	0.757 ± 0.006	-50.2 ± 22.4
83	00:43:28.60	+41:14:36.7	14.059 ± 0.001	0.817 ± 0.002	2.051 ± 0.002	33.7 ± 30.9
84	00:43:33.22	+40:53:06.8	15.805 ± 0.002	0.730 ± 0.004	1.725 ± 0.006	-36.4 ± 20.5
85	00:43:48.62	+40:30:15.6	15.881 ± 0.002	0.675 ± 0.004	1.447 ± 0.005	3.8 ± 30.5
86	00:43:52.15	+40:22:28.5	15.820 ± 0.002	0.662 ± 0.004	1.415 ± 0.004	-148.2 ± 28.9
87	00:44:10.48	+41:58:19.0	16.379 ± 0.005	0.559 ± 0.008	1.114 ± 0.011	-44.8 ± 38.4
88	00:44:13.12	+41:55:07.1	15.826 ± 0.003	0.626 ± 0.005	1.378 ± 0.008	-57.2 ± 38.5
89	00:44:14.88	+40:28:46.6	16.046 ± 0.002	0.813 ± 0.004	1.934 ± 0.007	-40.3 ± 30.9
90	00:44:19.78	+41:55:59.3	18.452 ± 0.034	1.001 ± 0.068	1.763 ± 0.110	-62.3 ± 52.2
91	00:44:27.77	+41:34:05.5	15.167 ± 0.003	0.624 ± 0.004	1.327 ± 0.004	-111.3 ± 28.7
92	00:45:09.49	+40:38:17.8	16.903 ± 0.005	0.581 ± 0.008	1.161 ± 0.009	-201.9 ± 41.1
93	00:45:12.18	+40:36:37.7	16.007 ± 0.002	0.447 ± 0.004	0.741 ± 0.004	-67.7 ± 56.7
94	00:45:25.57	+41:01:23.7	17.471 ± 0.008	0.616 ± 0.013	1.576 ± 0.019	31.0 ± 28.3
95	00:45:49.73	+41:31:19.9	15.150 ± 0.002	0.599 ± 0.003	1.293 ± 0.003	-21.5 ± 35.1
96	00:46:41.79	+40:25:57.6	16.956 ± 0.005	0.816 ± 0.009	1.833 ± 0.014	-80.8 ± 26.6
97	00:46:43.13	+40:39:33.5	16.881 ± 0.005	0.599 ± 0.008	1.314 ± 0.010	-1.8 ± 27.0
98	00:46:50.46	+40:39:19.7	18.101 ± 0.014	0.913 ± 0.027	2.196 ± 0.054	37.8 ± 63.3
99	00:47:06.86	+40:37:00.1	15.102 ± 0.001	0.738 ± 0.002	1.704 ± 0.003	-56.1 ± 36.3
100	00:47:15.52	+40:36:57.8	18.658 ± 0.021	0.637 ± 0.034	1.462 ± 0.047	-126.9 ± 26.4
101	00:47:54.25	+40:46:07.7	17.207 ± 0.007	0.737 ± 0.011	1.714 ± 0.015	-63.7 ± 24.3
102	00:47:59.48	+41:48:49.0	16.231 ± 0.003	0.833 ± 0.007	2.001 ± 0.014	-27.9 ± 30.1
103	00:48:05.24	+41:49:50.4	16.560 ± 0.005	0.604 ± 0.008	1.352 ± 0.012	-113.4 ± 35.2

TABLE 8 — *Continued*

R.A. <sup>a</sup>		Decl. <sup>b</sup>		$v$			
ID	(J2000.0)	(J2000.0)	$T_1$	$(M-T_1)$	$(C-T_1)$	$(\text{km s}^{-1})$	
(1)	(2)	(3)	(4)	(5)	(6)	(7)	
104	00:48:07.05	+41:29:00.5	$15.420 \pm 0.002$	$0.643 \pm 0.003$	$1.447 \pm 0.005$	$-7.7 \pm 31.4$	
105	00:48:07.63	+41:57:57.5	$17.771 \pm 0.013$	$0.832 \pm 0.026$	$1.684 \pm 0.044$	$-28.1 \pm 35.9$	
106	00:48:15.84	+41:38:28.6	$15.745 \pm 0.002$	$0.590 \pm 0.004$	$1.250 \pm 0.005$	$-17.1 \pm 31.8$	
107	00:48:17.30	+41:22:16.6	$15.637 \pm 0.002$	$0.497 \pm 0.003$	$1.082 \pm 0.004$	$-36.2 \pm 44.5$	
108	00:48:32.47	+41:22:59.2	$16.810 \pm 0.005$	$0.515 \pm 0.009$	$1.019 \pm 0.011$	$-78.1 \pm 34.1$	
109	00:48:44.97	+41:23:11.5	$15.701 \pm 0.002$	$0.566 \pm 0.004$	$1.163 \pm 0.005$	$-136.2 \pm 24.9$	
110	00:48:59.44	+41:28:11.5	$16.053 \pm 0.003$	$0.598 \pm 0.005$	$1.257 \pm 0.007$	$-31.1 \pm 22.1$	
111	00:49:16.87	+41:00:58.1	$18.706 \pm 0.002$	...	...	$-46.0 \pm 43.5$	

NOTE. — Table 8 is published in its entirety in the electronic edition of the *Astronomical Journal*. A portion is shown here for guidance regarding its form and content.

<sup>a</sup> Right ascension in units of hours, minutes, and seconds.

<sup>b</sup> Declination in units of degrees, arcminutes, and arcseconds.

TABLE 9  
A LIST OF GALAXIES IDENTIFIED IN THIS STUDY

R.A. <sup>a</sup>		Decl. <sup>b</sup>		$v$				
ID	(J2000.0)	(J2000.0)	$T_1$	$(M-T_1)$	$(C-T_1)$	$(\text{km s}^{-1})$		RBC2 ID <sup>c</sup>
(1)	(2)	(3)	(4)	(5)	(6)	(7)	(8)	
1	00:36:32.94	+40:24:52.7	$16.408 \pm 0.004$	$0.788 \pm 0.006$	$1.849 \pm 0.009$	$10779.3 \pm 51.1$		B294
2	00:40:15.67	+41:48:30.4	$17.252 \pm 0.008$	$0.841 \pm 0.014$	$1.835 \pm 0.022$	$53856.7 \pm 68.2$		B320
3	00:40:27.23	+41:29:09.1	$17.352 \pm 0.014$	$0.801 \pm 0.018$	$1.705 \pm 0.023$	$41878.8 \pm 69.1$		B007
4	00:40:55.18	+41:57:28.7	$17.695 \pm 0.011$	$0.881 \pm 0.021$	$2.174 \pm 0.041$	$35348.9 \pm 74.1$		...
5	00:41:00.13	+41:55:39.8	$16.972 \pm 0.006$	$0.951 \pm 0.012$	$2.260 \pm 0.023$	$28551.8 \pm 65.7$		...
6	00:42:49.35	+41:59:06.6	$18.392 \pm 0.032$	$0.732 \pm 0.056$	$2.059 \pm 0.138$	$35984.0 \pm 100.3$		...
7	00:43:14.56	+40:22:58.9	$18.767 \pm 0.028$	$1.004 \pm 0.052$	$2.532 \pm 0.116$	$38863.2 \pm 89.3$		...
8	00:43:15.67	+42:01:47.9	$17.738 \pm 0.018$	$0.759 \pm 0.031$	$2.045 \pm 0.075$	$22246.6 \pm 58.1$		...
9	00:43:47.30	+40:32:54.8	$17.900 \pm 0.011$	$0.986 \pm 0.022$	$2.040 \pm 0.036$	$52702.6 \pm 99.2$		...
10	00:44:52.40	+41:46:29.1	$19.630 \pm 0.095$	$-0.183 \pm 0.112$	$2.849 \pm 0.761$	$47585.2 \pm 41.2$		...
11	00:45:48.73	+41:02:14.0	$17.835 \pm 0.011$	$0.819 \pm 0.020$	$1.939 \pm 0.032$	$33179.9 \pm 107.0$		...
12	00:46:24.87	+41:35:09.1	$17.223 \pm 0.009$	$0.640 \pm 0.013$	$1.385 \pm 0.015$	$28367.1 \pm 80.7$		B385
13	00:46:29.20	+40:20:35.0	$17.658 \pm 0.009$	$0.869 \pm 0.016$	$2.057 \pm 0.029$	$35611.0 \pm 112.8$		...
14	00:46:43.77	+41:49:09.9	$16.840 \pm 0.008$	$1.022 \pm 0.015$	$2.516 \pm 0.039$	$37728.3 \pm 85.9$		B389
15	00:47:00.27	+40:59:38.0	$17.011 \pm 0.006$	$0.711 \pm 0.010$	$1.523 \pm 0.013$	$32027.7 \pm 60.1$		B299D
16	00:47:00.33	+40:40:36.7	$17.427 \pm 0.008$	$0.872 \pm 0.015$	$2.078 \pm 0.027$	$39567.8 \pm 67.8$		B300D
17	00:47:12.50	+41:30:07.7	$17.880 \pm 0.016$	$0.887 \pm 0.025$	$2.164 \pm 0.041$	$32632.9 \pm 89.6$		...
18	00:47:26.23	+41:47:41.4	$18.634 \pm 0.027$	$0.942 \pm 0.059$	$2.514 \pm 0.187$	$38498.4 \pm 102.2$		...
19	00:47:31.18	+41:52:59.7	$18.501 \pm 0.024$	$0.854 \pm 0.050$	$2.364 \pm 0.147$	$32383.9 \pm 105.4$		...
20	00:47:41.69	+41:46:41.4	$17.518 \pm 0.010$	$0.901 \pm 0.022$	$2.089 \pm 0.048$	$32408.5 \pm 78.0$		...
21	00:48:33.48	+41:43:44.4	$18.070 \pm 0.016$	$0.855 \pm 0.033$	$2.212 \pm 0.079$	$38208.4 \pm 113.9$		...

<sup>a</sup> Right ascension in units of hours, minutes, and seconds.

<sup>b</sup> Declination in units of degrees, arcminutes, and arcseconds.

<sup>c</sup> Identification in the Revised Bologna Catalogue V2.0 of Galleti et al. (2006)